Journal of Petroleum Science and Engineering 201 (2021) 108477

Contents lists available at ScienceDirect

Journal of Petroleum Science and Engineering

journal homepage: http://www.elsevier.com/locate/petrol

Identification of effective source rocks in different sedimentary environments and evaluation of hydrocarbon resources potential: A case study of paleogene source rocks in the Dongpu Depression, Bohai Bay Basin

Chenxi Zhu [a,b], Fujie Jiang [a,b,*], Pengyuan Zhang [d,e], Tao Hu [a,b], Ying Liu [a,b], Tianwu Xu [c], Yun-xian Zhang [c], Qian Deng [a,b], Yongshui Zhou [c], Hang Xiong [a,b], Zezhang Song [a,b]

[a] State Key Laboratory of Petroleum Resources and Prospecting, China University of Petroleum (Beijing), Beijing, 102249, China
[b] College of Geosciences, China University of Petroleum, Changping District, Beijing, 102249, China
[c] Zhongyuan Oilfield Branch, SINOPEC, Henan, 457001, China
[d] Key Laboratory of Cenozoic Geology and Environment, Institute of Geology and Geophysics, Chinese Academy of Sciences, Beijing, PR China
[e] University of Chinese Academy of Sciences, Beijing, PR China

ARTICLE INFO

Keywords:
Continental basin
Saline lacustrine basin
Effective source rock
Hydrocarbon expulsion threshold
Resource potential
Dongpu depression

ABSTRACT

Source rocks in lacustrine rifting basins have great heterogeneity, which leads to imprecise assessments of hydrocarbon resources. Previous studies evaluated the source rocks of different sedimentary environments in lacustrine basins or depressions using the same lower limit of effective source rocks (i.e., the minimum total organic carbon (TOC) at which the source rocks are capable of expelling hydrocarbons). In this study, the source rock samples were selected from five formations in the Dongpu Depression for organic geochemical experiments and quantitative simulations of hydrocarbon expulsion. According to salinity differences, every formation was divided into a saline area, transition area and freshwater area. The results show that the maximum thickness of source rocks developed in the saline and transition areas is 700 m. Additionally, source rocks with a higher TOC and oil-prone organic matter types (II_1 and II_2) also develop in the saline and transition areas, and most have entered the mature stage. The TOC values corresponding to the lower limit of effective source rocks in the saline, transition, and freshwater areas are 0.3%, 0.4% and 0.5%, respectively. Furthermore, the hydrocarbon expulsion ratio (amount of hydrocarbon discharged per unit of TOC from the source rocks) for the freshwater area is 253.1 mg/g, while the ratios in the saline and transition areas are relatively higher at 439.4 mg/g and 369.3 mg/g, respectively. The hydrocarbon expulsion rate (change in the expulsion ratio per unit thermal evolution degree) and hydrocarbon expulsion efficiency (ratio of cumulative hydrocarbon expulsion amount to generation amount) in the saline, transition and freshwater areas present maxima when the Ro (vitrinite reflectance) values are 0.95%, 0.85% and 0.82%, respectively. The hydrocarbon expulsion quantities in the saline, transition and freshwater areas account for 24%, 49% and 27% of the total, respectively. Therefore, the main hydrocarbon expulsion area is the transition area of the Dongpu Depression associated with the thickest source rocks. Es_3^M and Es_3^L source rocks in the transition area with high organic matter abundant and type II kerogen are more promising than the other formations. This study is the first to report on effective source rocks in different sedimentary environments in lacustrine basins and can provide guidance for future exploration in the Dongpu Depression and a reference for future research on source rocks in other lacustrine basins.

1. Introduction

Although most of the world's oil and gas resources are concentrated in marine basins, lacustrine basins contribut 20% of the world's total reserves (Perotti et al., 2016; Konyuhov et al., 2006; Zou et al., 2019; Lu et al., 2017). In China, India and Brazil, lacustrine basins are the major oil and gas production bases and contribute more than 85% of the oil and gas reserves (Smith et al., 1978; Zheng et al., 2019; Atmaram et al., 2018; Kumar et al., 2017; Weng et al., 2010; Mosmann et al., 1984; Wang et al., 2002; Jiang et al., 2016; Hu et al., 2021, 2018). Compared

* Corresponding author. State Key Laboratory of Petroleum Resources and Prospecting, China University of Petroleum (Beijing), Beijing, 102249, China.
E-mail address: jfjhtb@163.com (F. Jiang).

https://doi.org/10.1016/j.petrol.2021.108477
Received 22 October 2019; Received in revised form 20 January 2021; Accepted 25 January 2021
Available online 4 February 2021

Table 1
Geochemical characteristics of Lacustrine basins with different salinity.

Basin	Fm.	$\delta^{13}C$ (‰)	Sp (‰)	TOC (%)	S_1 (%)	Lower limit of effective source rock	Reference
Dongying Depression	Es_3^l	–	12.40	4.47	3.81	TOC>1.5%	[21,31,38]
	Es_4^u	–	31.00	3.36	4.63	TOC>1.5%	
Qaidam Basin	E_3	–	11.50	0.3–0.6	–	TOC>0.4%	[32,33,39]
	E_{1+2}	–	9.30	–	–	TOC>0.4%	
Dongpu Depression	Es_3^u	–	10.38	0.97	–	–	[40]
	Es_3^l	–	11.56	0.89	–	–	
Songliao Basin	K_2n^1	−25~-31	–	0.24–12	–	TOC>0.5%	[34,35]
	K_2n^2	−29~-26	–	0.93–4.3	–	TOC>0.5%	
Ordos Basin	Chang-9	–	5.00	3.05	–	TOC>1.1%	[14,36,37]
Note:	Fm.: Formation						

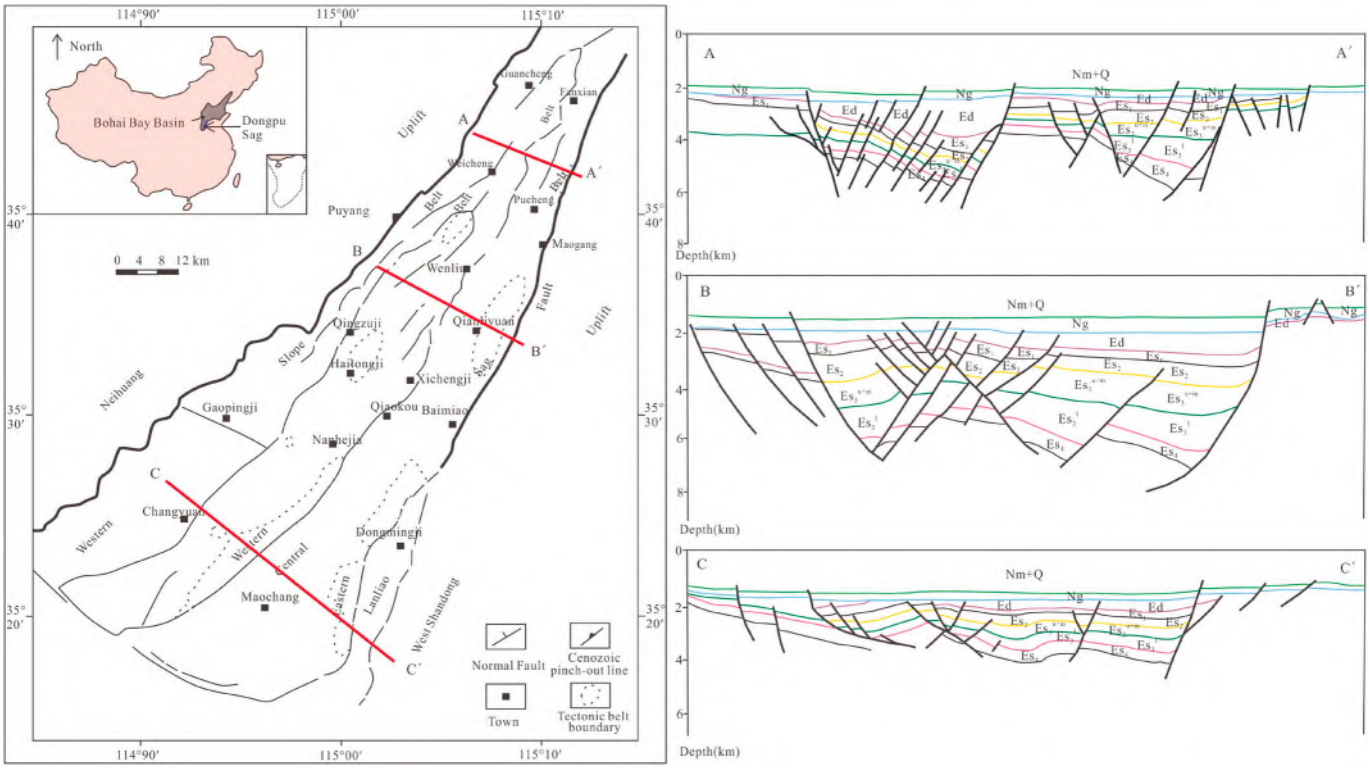

Fig. 1. Structure map of Dongpu Depression in the Bohai Bay Basin and representative cross section (modified from Oilfield, 1993; Liu and Jiang, 2013; Zhang et al., 2015).

with marine basins, the sedimentary process of lacustrine basins is greatly affected by the paleoclimate and paleoenvironment and by the frequency of lacustrine invasions and regressions, leading to variable sedimentary types in a small area, and several completely different sedimentary environments often occur within a secondary tectonic unit (Ribes et al., 2015; Aziz et al., 2003; Thiry et al., 1989). Therefore, the source rocks are heterogeneous and present uneven thicknesses in the horizontal plane as well as sharp variations in vertical lithology (Yurchenko et al., 2018; Pu et al., 2015; Fan et al., 2018; Hakimi et al., 2016). In such cases, the study of source rocks becomes complicated. Several scholars have studied source rocks in lacustrine basins (Harris et al., 2004; Sykes et al., 2002; Petersen et al., 2006) and showed that the source rocks in saline lacustrine basins are quite different from those in freshwater lacustrine basins and that the quality of the source rocks varies with the degree of salt content (Zhao et al., 2003; Wang et al., 2020a, 2020b, 2020c; Ma et al., 2018; Zhang et al., 2021; Zhu et al., 2003; Huo et al., 2020; Lu et al., 2011). However, the traditional evaluation process, which ignores various environments, is still used to assess the quality and effectiveness of the source rocks deposited with different salinity levels (Table 1). In this study, effective source rock is defined as the source rock that expelled the hydrocarbons during the hydrocarbon generation process of organic matter (Peters et al., 2005). For example, the paleosalinity of the Es_3^L and Es_4^U source rocks in the Dongying Depression is 12.4‰ and 31‰, respectively, but the lower limit of effective source rocks is the same, with total organic carbon (TOC) > 1.5% (Liang et al., 2018a, 2018b; Wei et al., 2018). The heterogeneity of the source rocks was not considered in these assessments, which led to inaccurate evaluations of the potential of oil and gas resources in lacustrine basins. Therefore, the identification of effective source rocks of different sedimentary environments is important for oil and gas exploration and resource evaluation (He et al., 2018; Magnier et al., 2004).

The Dongpu Depression, which is rich in oil and gas resources and has a proven resource amount of 5×10^8t, is a typical lacustrine rift basin in eastern China. Some studies have predicted the future exploration and development area of the Es_3 (the third member of the Shahejie Formation) of the Dongpu Depression, and it is believed that there may be complex oil and gas reservoirs in the Qianliyuan and Haitongji-Liutun areas (Zhu et al., 2010). For unconventional resources, the lower limits of hydrocarbon generation of the source rocks in the south (Ro

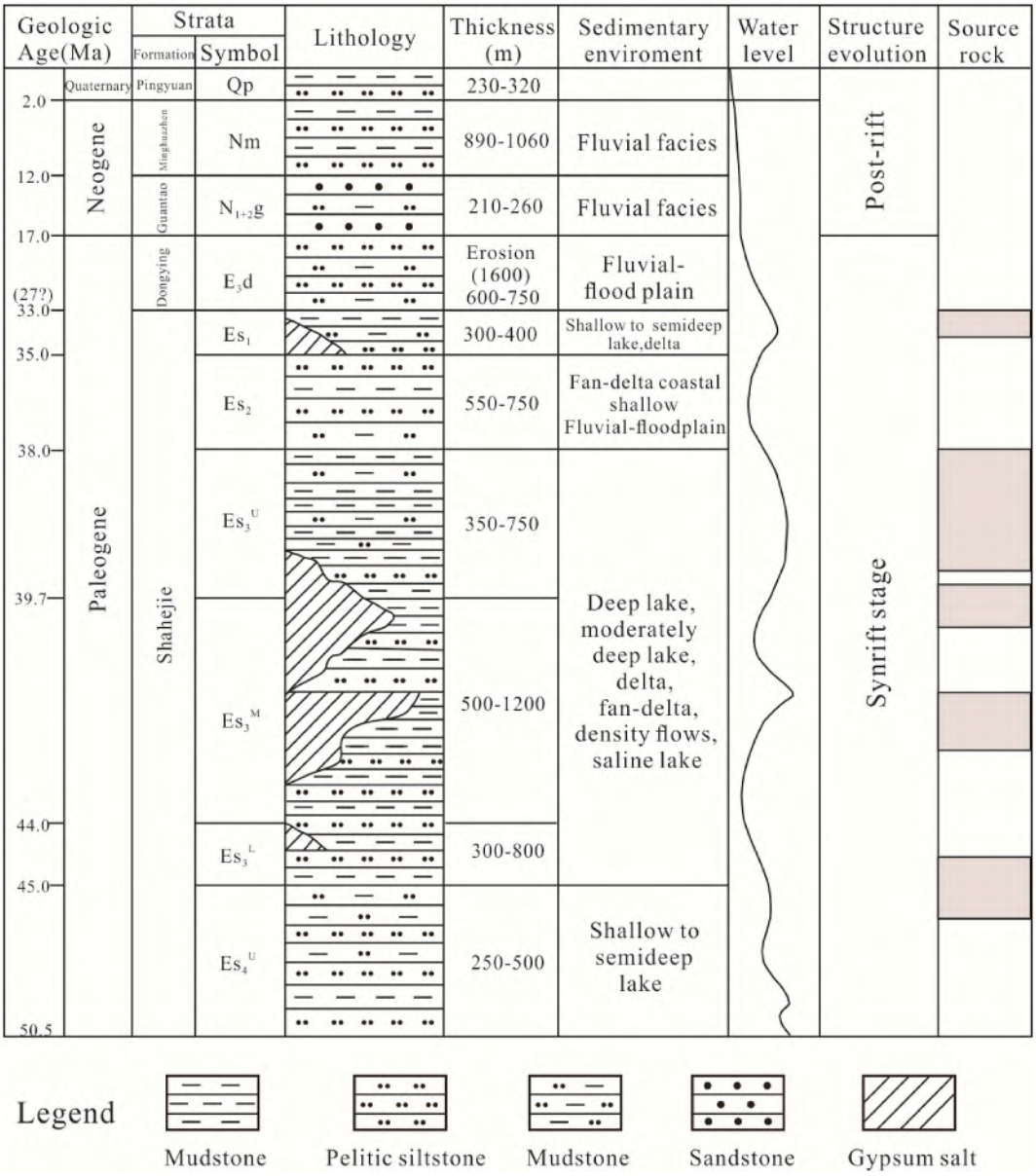

Fig. 2. Generalized stratigraphy of Dongpu Depression (modified from Oilfield, 1993; Lu et al., 1993; Liu and Jiang, 2013; Zhang et al., 2015; Huang et al., 2018).

value is 3.20%–3.74%) and north (Ro value is 3.61%–3.97%) were determined, and the amount of hydrocarbon generation was less than 1% of the total when exceeding this lower limit (Tang et al., 2019). In previous studies, three different sedimentary environments were developed in the plane with different salinities and similar tectonic histories and burial histories in the Dongpu Depression, which are the saline area (salinity value is 0.38%–2.29% with a mean value of 1.1.8%), transition area (salinity value is 0.66%–1.20% with a mean value of 0.90%) and freshwater area (salinity value is 0.61%–1.02% with a mean value of 0.85%) (Ji et al., 2018; Zuo et al., 2017; Hu et al., 2018). In addition, 93.7% of the oil and over 80% of the natural gas are distributed in the north, where the saline and transition areas are situated (Wang et al., 2020a, 2020b, 2020c; Liu et al., 2014), while only a small amount of oil and gas resources are distributed in the freshwater area. Studies on the source rocks in the Dongpu Depression show that the lithologic and organic geochemical characteristics in the saline, transition and freshwater areas are greatly different (Lyu et al., 2019; Zheng et al., 2020; Wu et al., 2000; Bian et al., 2020; Chen et al., 2018). However, there are still three problems: (1) the effectiveness of the source rocks in different sedimentary environments of lacustrine basins has not been discussed in previous studies (Klemme et al., 1991; Hakimi et al., 2020); (2) the contribution of hydrocarbon expulsion quantity of the source rocks developed in different sedimentary environments relative to the total hydrocarbon expulsion quantity is not clear; (3) previous studies were limited to source rocks in a single formation or a single region in the Dongpu Depression (Wu et al., 2000; Yue et al., 2005; Lyu et al., 2019; Bian et al., 2020) and did not perform systematic studies of the source rocks in the Dongpu Depression.

In this study, the hydrocarbon resources potential of three different sedimentary environments in different formations of the Paleogene Shahejie Formation are evaluated using the organic geochemical data, including TOC, Rock-Eval pyrolysis, vitrinite reflectance Ro, chemical element composition and macerals. The weighted average method is used to deal with geochemical data of different depths in a single well (Jiang et al., 2016). Based on the principle of material balance (when organic matter does not exchange energy of any form with the outside world during the hydrocarbon generation and expulsion process, the total amount of organic matter is invariable), the hydrocarbon

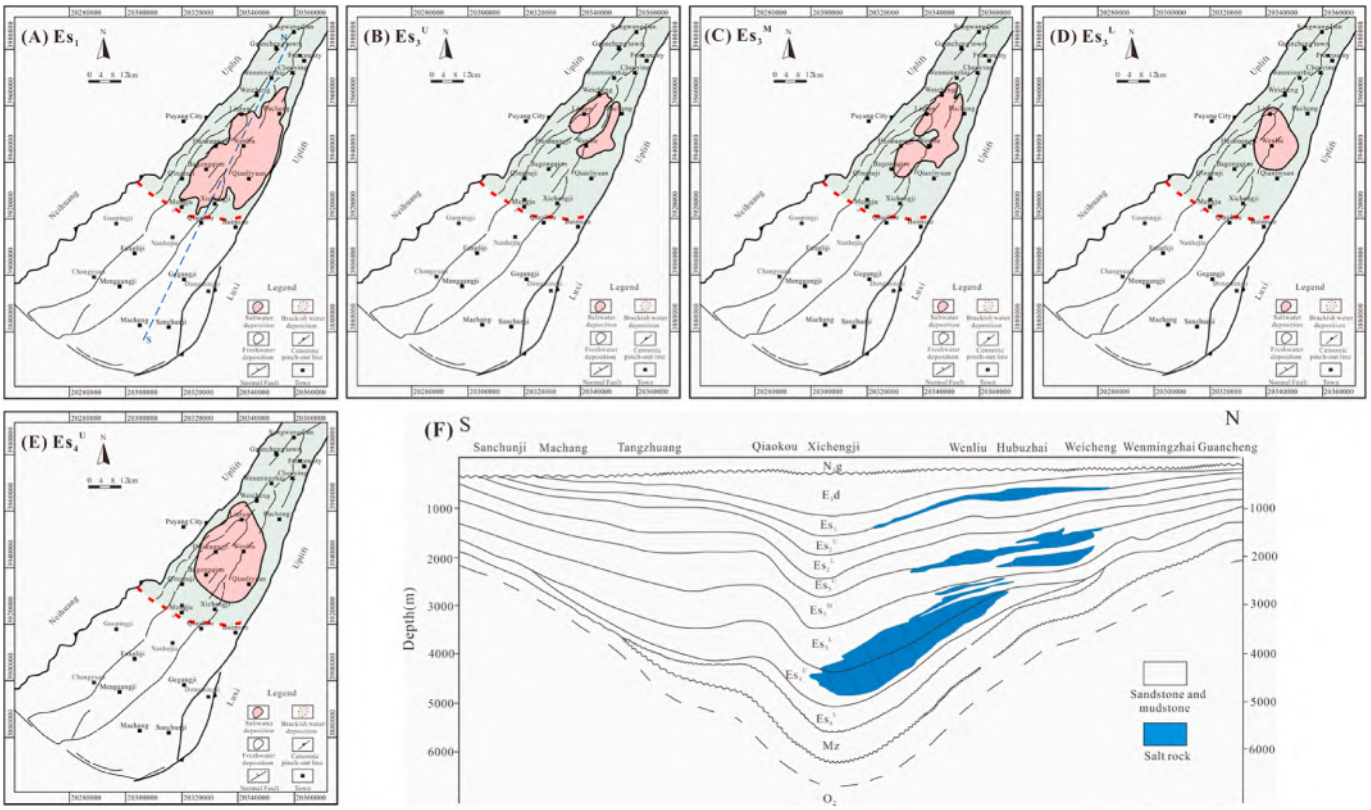

Fig. 3. Horizontal and vertical distribution of salt-bearing strata in Dongpu Depression of the Bohai Bay Basin: (a) first member of the Shahejie Formation (Es_1), (b) upper third submember of the Shahejie Formation (Es_3^U), (c) middle third submember of the Shahejie Formation (Es_3^M), (d) lower third submember of the Shahejie Formation (Es_3^L), (e) upper fourth submember of the Shahejie Formation (Es_4^U), and (f) vertical distribution of salt-bearing strata (modified from Oilfield, 1993; Mu, 2011).

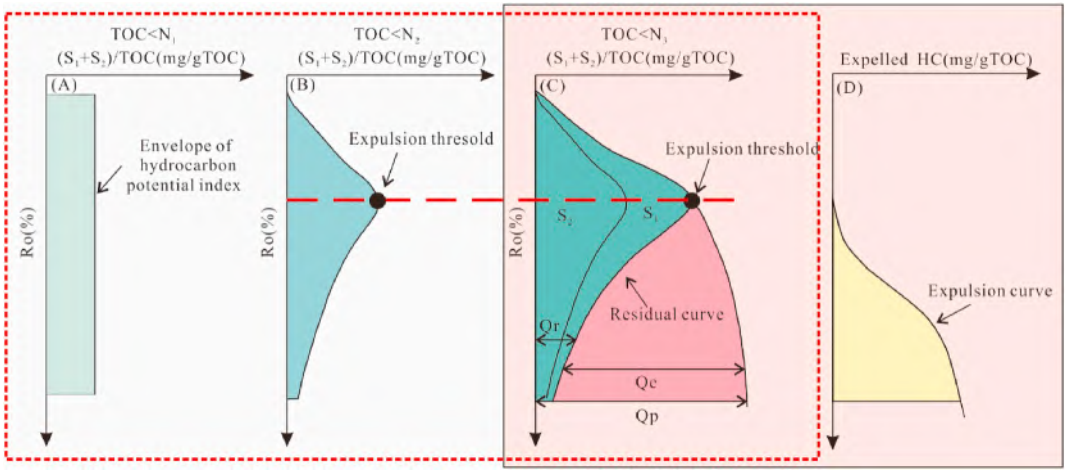

Fig. 4. Simple conceptual model of source rock hydrocarbon generation and expulsion features. (A), (B) and (C) Models used to identify the lower threshold of the effective source rock; (C) and (D) source rock hydrocarbon generation and expulsion features. N_1, N_2 and N_3 are the total organic carbon content, and N_1 is the lower threshold of the effective source rock (modified from Xiongqi Pang, 1995; Li et al., 2018).

generation potential method, which has been applied in many petroliferous basins in China (Bai et al., 2017; Hu et al., 2015; Peng et al., 2018; Wang et al., 2020a, 2020b, 2020c; Zhu et al., 2020), is used to identify the effective source rocks and analyze the hydrocarbon expulsion characteristics (Pang et al., 1995). By taking source rocks developed in different lacustrine sedimentary environments as examples, this study aimed at (1) investigating the geochemical characteristics of different sedimentary environments from five source rock formations in the Paleogene, (2) identifying the lower limit of effective source rocks of different sedimentary environments, (3) clarifying the hydrocarbon expulsion characteristics of effective source rocks of different sedimentary environments, (4) making a comparison of the hydrocarbon expulsion amount from different sedimentary environments and guiding the future exploration direction.

2. Geological background

The Dongpu Depression is located in the southwest of the Bohai Bay

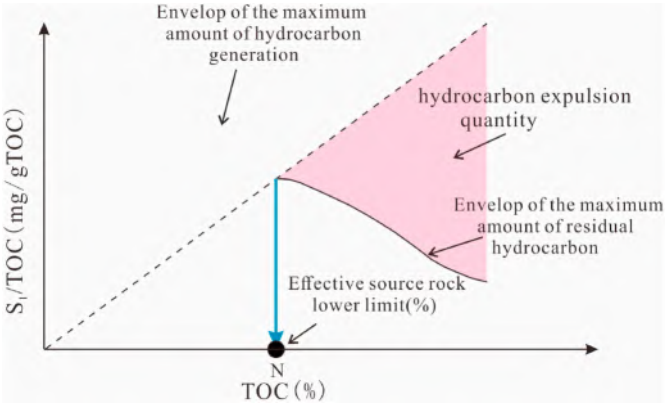

Fig. 5. Discriminant model diagram of the lower limit of hydrocarbon organic carbon content in effective source rocks (modified from Gang Gao et al., 2012).

Basin and has an NNE trend. The depression is located between the Neihuang uplift and Luxi uplift and widens in the south and narrows in the north, characteristic of a typical lacustrine rift basin. During the tectonic evolution, the tectonic pattern of "Two depressions, one uplift and one slope" was developed (Wang et al., 2015; Zuo et al., 2017) (Fig. 1).

The Bohai Bay Basin experienced three stages of evolution, and the Dongpu Depression formed during the second stage (50 Ma, Cenozoic). The tectonic evolution of the Dongpu Depression can be divided into the Paleogene rifting stage and Neogene depression stage. More specifically, the Paleogene rifting stage can be divided into (1) the initial rifting period (depositional period of the fourth member of the Shahejie Formation (Es_4)), (2) the main rifting period (depositional period of the third member of the Shahejie Formation (Es_3)), (3) the succession and development period (depositional period of the first and second members of the Shahejie Formation (Es_1 and Es_2)), and (4) the subsidence period (depositional period of the Dongying Formation (Ed)) (Shao et al., 2018).

The sedimentary environments of the five sets of source rocks that developed in the Dongpu Depression are quite different. The source rocks of Es_4^U (upper fourth submember of the Shahejie Formation) are distributed in the bottom formation of Paleogene age in the study area, with the deepest burial depth reaching approximately 10,000 m (~32,800 ft) and the thickness ranging from 250 to 500 m (820–1640 ft). From north to south, the meandering river delta plain, meandering river delta front, semi-deep lake, shore-shallow lake and delta front sedimentary facies developed successively. Es_3^L (lower third submember of the Shahejie Formation) source rocks experienced a short depositional period with a stratum thickness of 300–550 m (984–1804 ft). During this period, the meandering river delta-lake sediment were mainly deposited, and the distribution range of lacustrine facies gradually shrank. Additionally, the characteristics of "east-west zonation and north-south zonation" in the Dongpu Depression began to form in this period. The maximum thickness of Es_3^M (middle third submember of the Shahejie Formation) source rocks is 500–750 m (1640–2460 ft). The range of the meandering river delta plain and front facies expanded, and that of lacustrine facies continuously narrowed and gradually migrated northward. The thickness of Es_3^U (upper third submember of the Shahejie Formation) source rocks is 350–450 m (1148–1476 ft). During this period, the area of the delta plain and the delta front increased slightly, and that of the lacustrine facies further narrowed. During the deposition of Es_1 (first member of the Shahejie Formation), source rocks with a thickness of 300–400 m (984–1312 ft), the northern lake became deeper, and the spreading area of the delta sedimentary facies in the south expanded again. Finally, the delta-lake sedimentary system mainly developed in the Shahejie Formation of the Dongpu Depression, and the sedimentary environment of each formation of source rocks is quite variable due to frequent changes in the lacustrine level (Fig. 2).

Table 2
Strata thickness and source rock thickness of different sedimentary facies at different formations.

Fm.	Sedimentary Facies	No.	Range of strata thickness (m) / Average of strata thickness (m)	Range of source rock thickness (m) / Average of source rock thickness (m)
Es_1	Shore-shallow lake	40	153–498 303.86	100.5–378 212.62
	Meandering river delta leading edge	14	79–446 275.21	34.5–322 179.48
	Delta front	29	138–3220 1119.53	117–391 218.63
	Fan delta front	1	2495 2495.00	211 211.00
	Beach bar	1	342 342.00	252.5 252.50
	Saline lake	13	245–438 351.69	143.5–250 196.49
Es_3^U	Shore-shallow lake	42	187–3181 444.37	89.4–605 304.69
	Meandering river delta leading edge	13	183–490 292.38	0–259.5 106.48
	Delta front	134	136–1826 358.76	0 0.00
	Saline lake	7	239–370 310.14	189–285.2 237.33
Es_3^M	Shore-shallow lake	26	402–1633 696.62	236.5–1313.4 515.83
	Meandering river delta leading edge	11	233–804 487.91	142.5–604.7 319.94
	Meandering river delta plain	6	241–580 399.00	79–366 201.08
	Outer leading edge of meandering river delta	7	357–687 505.00	240.5–384.5 301.87
	Delta front	33	356–863 603.06	47.5–605 393.96
	Turbidite fan	1	846 846.00	699.9 699.90
Es_3^L	Shore-shallow lake	9	220–736 429.11	143.9–558.5 320.81
	Delta front	88	175–3935 724.01	70–674.9 330.98
	Saline lake	2	257–716 486.50	183.4–436.33 309.87
Es_4^u	Braided river delta inner leading edge	4	259–798 474.50	157.5–598.75 338.44
	Shore-shallow lake	1	402.5 402.50	343 343.00
	Meandering river delta leading edge	8	81–407 189.75	34–264.5 111.77
	Meandering river delta plain	4	168–651 402.00	107–320.5 205.25
	Delta front	40	46–583 224.58	31–454.5 130.90
	Salt lake	7	222–1110 536.29	111.5–626 281.36

Note: Fm.: Formation, N: Number of wells.

Shore-shallow lacustrine and semi-deep lacustrine sedimentary facies developed in the northern Dongpu Depression (Mu, 2011; Yang et al., 2019), which led to the deposition of thick-layered gypsum-salt rocks distributed in Es_4^U, Es_3^L, Es_3^M, Es_3^U and Es_1 vertically (Fig. 3f). The distribution differs among the five formations of gypsum-salt rocks. The Es_4^U salt rocks are located between eastern Wuxingji and western Qianliyuan and reach Mazhai in the north and the Xichengji area in the south, and the range of the salt rocks is elliptical (Fig. 3e). The salt rocks of Es_3^L are located in Liutun, Huzhuangji and Qianliyuan (Fig. 3d). Es_3^M salt rocks mainly are distributed in Huzhuangji, Mazhai and Pucheng, and they reach Wenmingzhai in the north and Qianliyuan in the south (Fig. 3c). Es_3^U salt rocks are mainly located in the areas near Liutun, Qiandugu, Wenliu and Pucheng (Fig. 3b). The range of Es_1 salt rocks is larger than those of other formations, reaching Chenying and Wenming

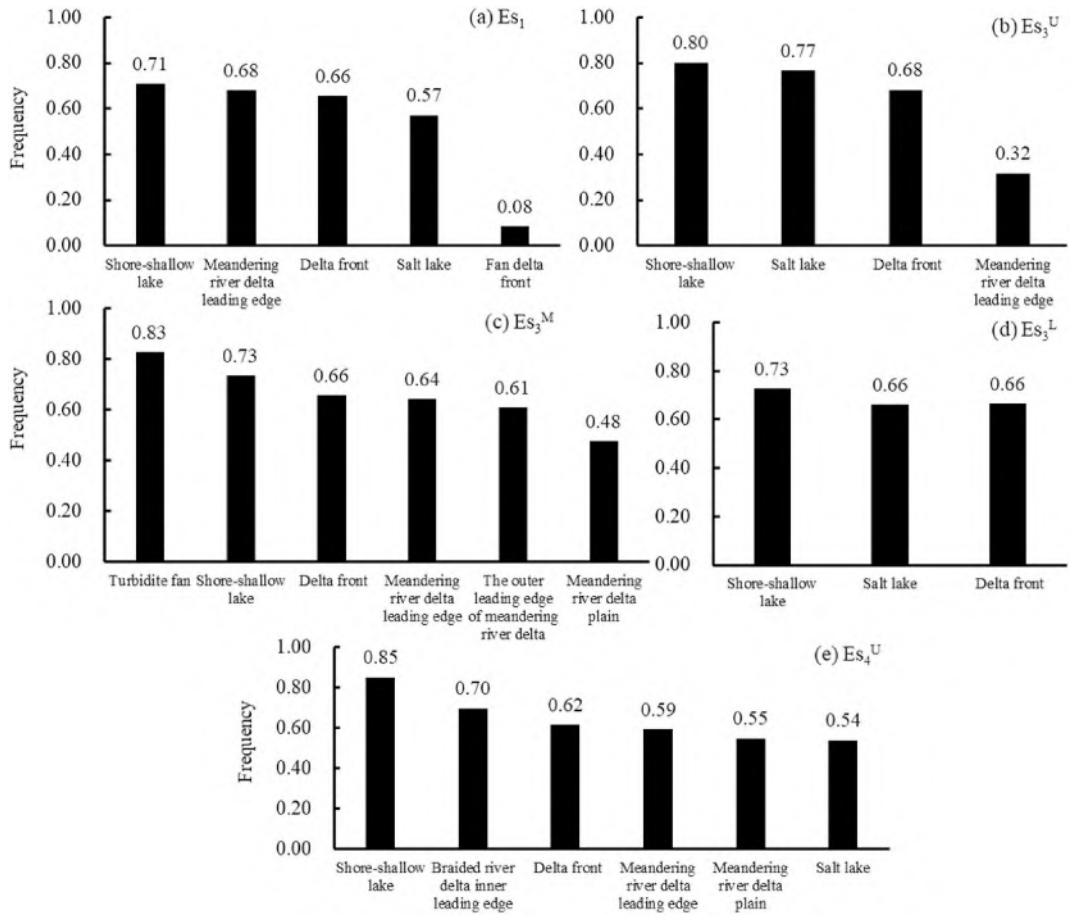

Fig. 6. Correlation between the source rock thickness/the strata thickness ratio and facies of individual source rocks in the Dongpu Depression: (a) first member of the Shahejie Formation (Es_1), (b) upper third submember of the Shahejie Formation (Es_3^U), (c) middle third submember of the Shahejie Formation (Es_3^M), (d) lower third submember of the Shahejie Formation (Es_3^L), and (e) upper fourth submember of the Shahejie Formation (Es_4^U).

in the north, Mengju and Qiaokou in the south, the Liutun and Huzhuangji areas in the west, and the Lanliao fault in the east (Fig. 3a).

3. Samples and methods

3.1. Samples

In this study, 513 samples of five formations distributed in the saline area, transition area and freshwater area were selected from 25 key wells for geochemical experiments. According to the core observations, the lithology of the source rocks is mainly dark mudstone, shale, sandy and silty shale, saline shale and dark oil shale. In addition, more than 3000 experimental data provided by Sinopeo Zhongyuan Oilfield Exploration and Development Research Institute were used to establish the hydrocarbon expulsion model, lending credibility to the results.

3.2. Laboratory method

The experiments mainly included the analysis of the pyrolysis, TOC, chemical element composition, vitrinite reflectance and macerals. The experimental data are shown in Table 5.

A LECO CS-230 analyzer (GB/T19145-2003 standard procedure) was used to test the TOC content. A 12.5% hydrochloric acid solution was slowly added to the powdered samples weighing approximately 10 mg, and the samples were kept at 60 °C for more than 2 h until the end of the reaction. Finally, the samples were slowly washed with distilled water until the acidic solution was cleaned, and then the samples were cooled.

A Rock-Eval instrument was used for the rock pyrolysis experiment at the Zhongyuan Oilfield Exploration and Development Research Institute. The experimental samples were crushed to 100 mesh size, and the peak area when heated to 300 °C corresponded to volatile hydrocarbon S_1 (mg HC/g Rock); the samples were heated from 300 °C to 500 °C, corresponding to the peak area representing pyrolyzed hydrocarbon S_2 (mg HC/g rock). In the process of obtaining the S_2, the maximum pyrolysis temperature of the Rock-Eval II instrument is the maximum peak temperature of pyrolysis (T_{max}) (Peters and Cassa, 1994; Behar et al., 2001).

The element content of carbon, hydrogen and oxygen in the rock organic matter was determined with an elemental analyzer.

The microconstituents were determined with an MPV-SP microscope and a photometer. Thermal maturity was analyzed with a 308-PV microphotometer. The micro-components were determined using the transmission light fluorescence kerogen micro-component identification method.

4. Evaluation method

4.1. Evaluation of source rock

The maximum depth of the Shahejie Formation source rocks in the Dongpu Depression is over 4500 m (14,760 ft); therefore, few exploration wells have been drilled to this depth. In addition, the location of the source rocks is closely related to the types of sedimentary facies. Therefore, the sedimentary facies constraint method that combines the ratio of the source rock thickness to strata thickness in different sedimentary facies with the distribution of sedimentary facies can be used to

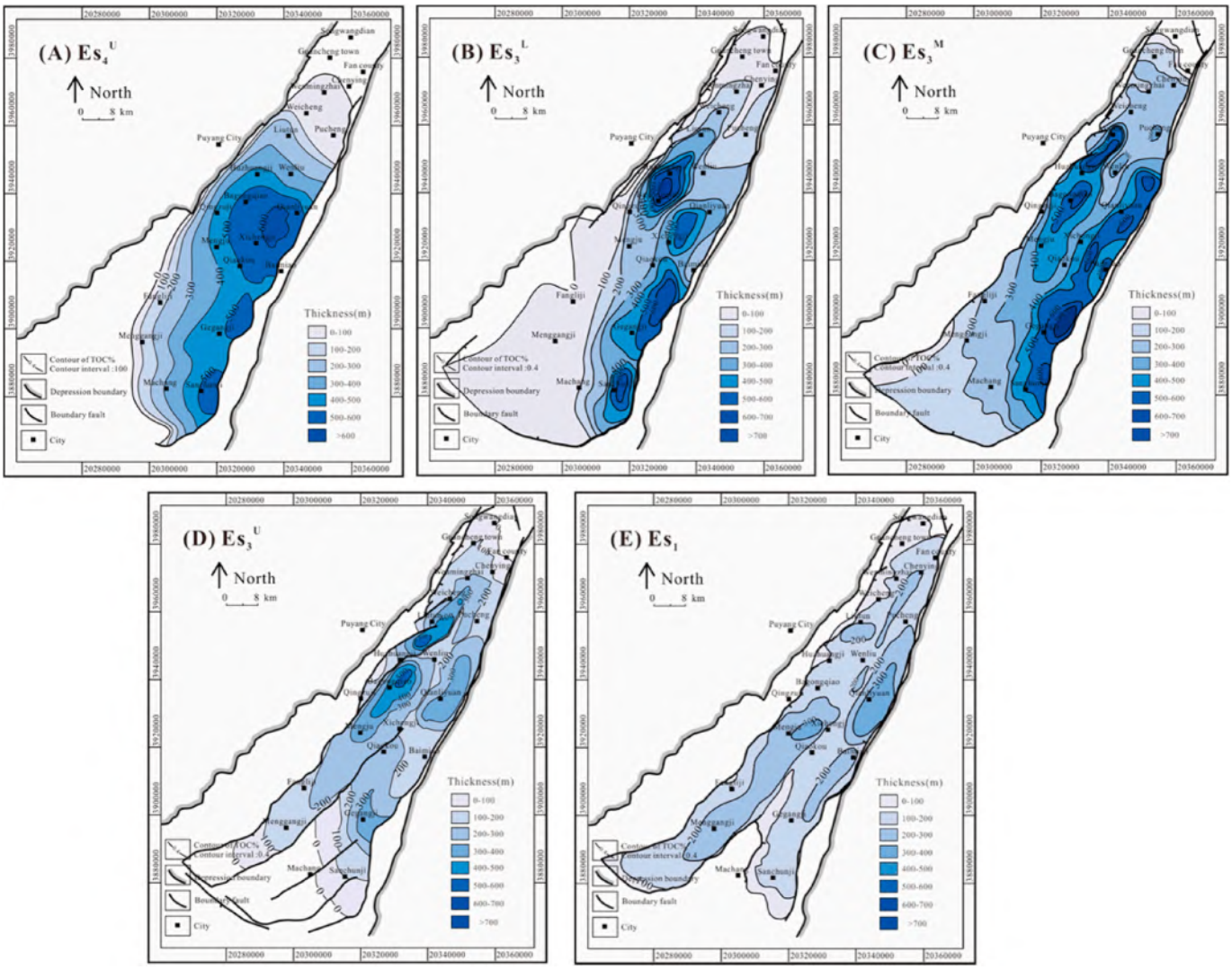

Fig. 7. Plane distribution of source rocks of the Shahejie Formation in the Dongpu Depression: (A) first member of the Shahejie Formation (Es_1), (B) upper third submember of the Shahejie Formation (Es_3^U), (C) middle third submember of the Shahejie Formation (Es_3^M), (D) lower third submember of the Shahejie Formation (Es_3^L), and (E) upper fourth submember of the Shahejie Formation (Es_4^U).

predict the thickness of the source rocks in areas with no drilled well (Jiang et al., 2016). In this study, the frequency histograms of this ratio in different sedimentary facies were established to help predict the distribution of the source rocks.

Currently, the most common method of calculating the value of the geochemical characteristic contours is the weighted average method, which can reduce the errors caused by the uneven distribution of the source rock thickness and geochemical data of the samples and improve the accuracy of the source rock evaluation (Jiang et al., 2010; Peters et al., 2006). The formula for this method is as follows:

$$X = (x_1 \times m_1 + x_2 \times m_2 + \ldots + x_n \times m_n)/(m_1 + m_2 + \ldots m_n) \quad (1)$$

where X represents the average geochemical parameter (i.e., TOC and Ro) value of a single well, x_n represents the parameter value of the n th measuring point in a single well, and m_n represents the thickness of a thin formation of the same lithology from the n th measuring point in a single well.

To make this study more intuitive and suitable for plane analysis and research, the interpolation method was used to predict the data of the contour lines such as the thickness data of dark mudstone, effective source rocks and geochemical data. Thus, the plane distribution of each formation was obtained to better evaluate the hydrocarbon source rocks.

4.2. Evaluation of hydrocarbon expulsion

4.2.1. Hydrocarbon potential method

The process of hydrocarbon potential generation is based on the principle of material balance, in which the mass of organic matter in source rocks remains unchanged before and after hydrocarbon generation and expulsion. In other words, if there is no energy exchange of any form with the external environment during the evolution process of source rocks, then the total amount of organic matter remains unchanged. Thus, the sum ($S_1 + S_2$) of volatile hydrocarbon (S_1) and pyrolyzed hydrocarbon (S_2) obtained by the rock pyrolysis (Rock-Eval) method represents the amount of hydrocarbon generation potential of the source rocks (P_g). In addition, the value of ((S_1+S_2)/TOC) represents the hydrocarbon generation potential index (P_g (Ro)), and then the relational diagram of (P_g (Ro)) and Ro compose the hydrocarbon potential index profile. The P_g (Ro) envelope line gradually increases with increasing Ro, and the Ro value is the hydrocarbon expulsion threshold when the P_g (Ro) is maximum. The hydrocarbon generation potential is called the initial hydrocarbon generation potential (HCI_o). When hydrocarbon expulsion begins, the P_g (Ro) envelope line gradually decreases, and the hydrocarbon generation potential is called the residual hydrocarbon generation potential (HCI_p) (Fig. 4C and D) (Pang et al.,

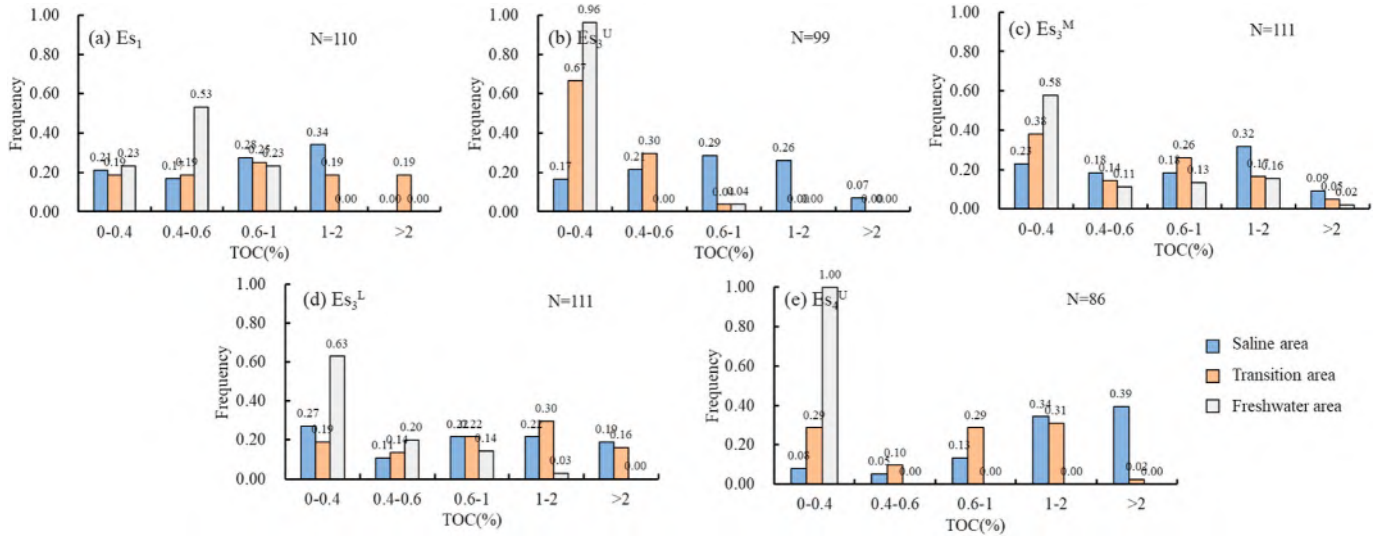

Fig. 8. Frequency distribution of total organic carbon in different sedimentary environments: (a) first member of the Shahejie Formation (Es_1), (b) upper third submember of the Shahejie Formation (Es_3^U), (c) middle third submember of the Shahejie Formation (Es_3^M), (d) lower third submember of the Shahejie Formation (Es_3^L), and (e) upper fourth submember of the Shahejie Formation (Es_4^U).

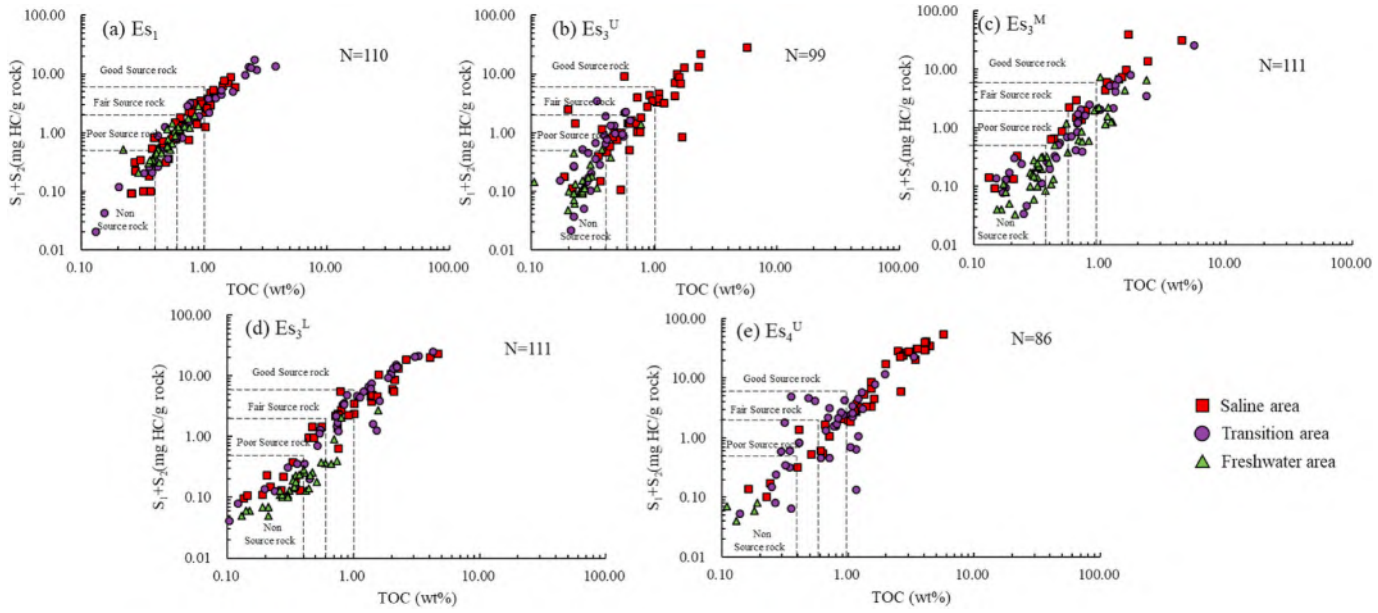

Fig. 9. S_1+S_2 vs TOC of the Shahejie Formation source rock in the Dongpu Depression: (a) first member of the Shahejie Formation (Es_1), (b) upper third submember of the Shahejie Formation (Es_3^U), (c) middle third submember of the Shahejie Formation (Es_3^M), (d) lower third submember of the Shahejie Formation (Es_3^L), and (e) upper fourth submember of the Shahejie Formation (Es_4^U).

2005).

The hydrocarbon expulsion ratio, the hydrocarbon expulsion rate and the hydrocarbon expulsion efficiency are calculated using the following Eqs. (2)–(4):

$$q_e = HCI_o - HCI_P \tag{2}$$

$$V_e = \Delta q_e / \Delta Ro \tag{3}$$

$$R_{eo} = q_e / HCI_o \times 100\% \tag{4}$$

where q_e represents the hydrocarbon expulsion ratio, which is the amount of hydrocarbon discharged per unit of organic carbon from the source rocks, mg/g; V_e represents the hydrocarbon expulsion rate, which is the change in the expulsion ratio per unit thermal evolution degree, mg/g/‰; and R_{eo} represents the hydrocarbon expulsion efficiency, which is the ratio of cumulative expulsion to cumulative generation amount, %.

Then, the hydrocarbon expulsion intensity can be calculated using Eq. (5), and the hydrocarbon expulsion quantities can be calculated using the following Eq. (6):

$$E_{hc} = \int_{Z_1}^{Z} q_e \times H \times \rho \times TOC \times dZ \tag{5}$$

$$Q_{hc} = E_{hc} \times S \tag{6}$$

where E_{hc} represents the hydrocarbon expulsion intensity, 10^3 t/km^2; Q_{hc} represents the hydrocarbon expulsion quantity, 10^3 t; Z represents

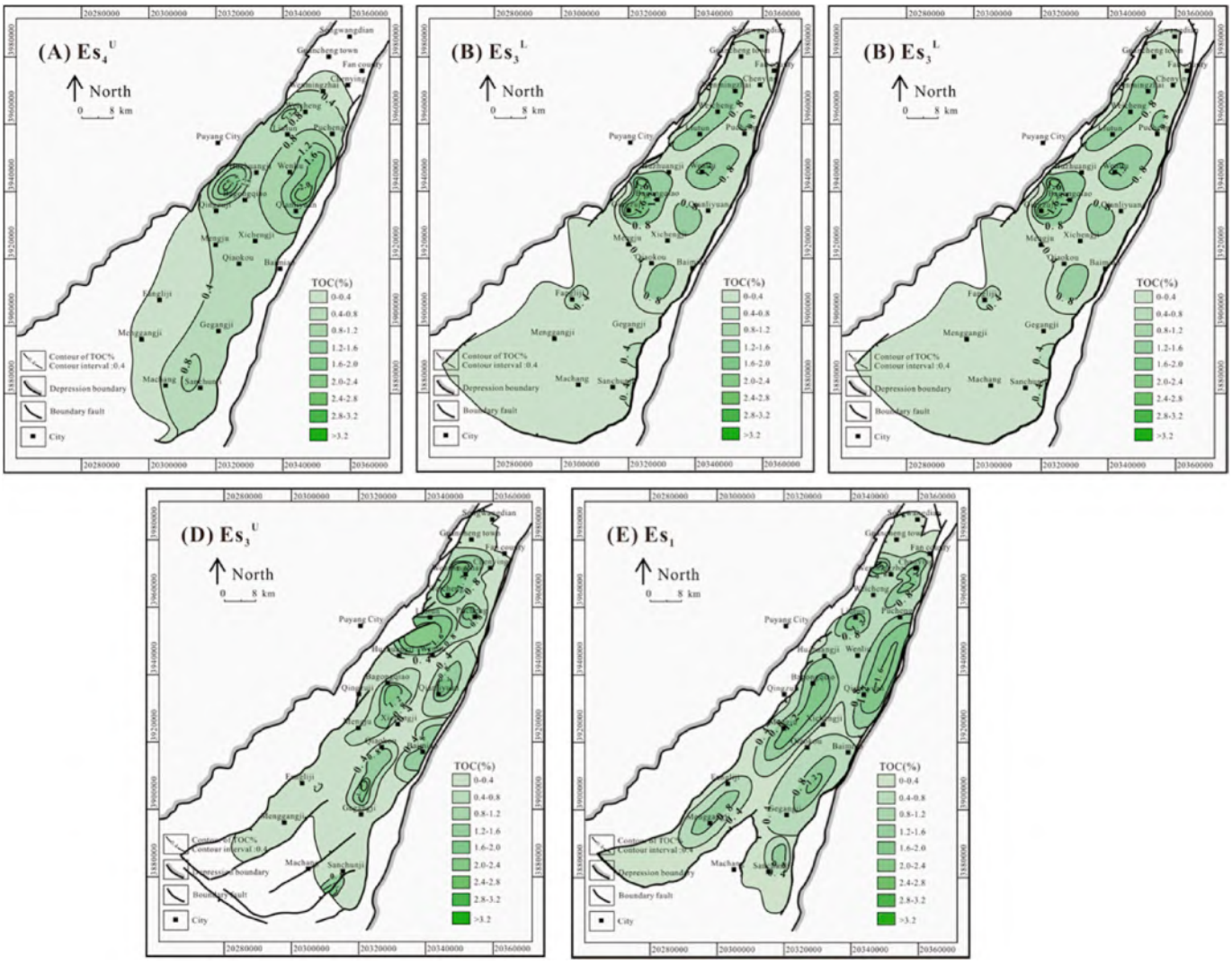

Fig. 10. Isopach of the total organic carbon abundance of the Shahejie Formation source rock in the Dongpu Depression: (A) first member of the Shahejie Formation (Es_1), (B) upper third submember of the Shahejie Formation (Es_3^U), (C) middle third submember of the Shahejie Formation (Es_3^M), (D) lower third submember of the Shahejie Formation (Es_3^L), and (E) upper fourth submember of the Shahejie Formation (Es_4^U).

the burial depth, m; Z_1 represents the depth corresponding to the hydrocarbon expulsion threshold, m; H represents the thickness of the source rocks, m; H represents the density of the source rocks, g/cm^3; and S is the source rocks area, m^2.

The hydrocarbon expulsion intensity map and the hydrocarbon expulsion quantity of different period can be obtained based on Eq. (5), Eq. (6) and the results of the source rock burial depth for different periods (Jiang et al., 2016).

4.2.2. Identification of effective hydrocarbon source rocks

(1) *Identifying effective source rocks by the hydrocarbon potential evolution profile*

Although some source rocks have reached the hydrocarbon expulsion threshold (Ro value of beginning hydrocarbon expulsion), they still cannot discharge hydrocarbons due to the low TOC content. Therefore, based on the hydrocarbon generation potential method, the hydrocarbon generation potential index profiles were established to identify the lower limits of TOC content in effective source rocks. When the envelopment line of the hydrocarbon generation potential index becomes curved, Pg (Ro) has a tendency of increasing first and then decreasing, meaning that hydrocarbons begin to discharge. Moreover, TOC = N_1 is the lower limit of the TOC content in effective source rocks (Pang et al., 1995) (Fig. 4A, B and C).

(2) *Identifying effective source rocks by the S_1 and TOC content*

Another method was selected to determine the lower limit of TOC content in effective source rocks (Gao et al., 2012). The residual organic matter is considered the amount of hydrocarbon generation when there is no expulsion of hydrocarbon in the source rocks. Moreover, with increasing TOC, the amount of hydrocarbon generation also increases. When TOC is greater than N, the hydrocarbon in the source rock after filling the pores of the rocks will be expelled from the source rock, and the maximum hydrocarbon generation amount begins to decrease; therefore, the envelope line of the maximum hydrocarbon generation amount will change to the envelope line of the maximum residual hydrocarbon. At this time, the corresponding TOC = N is the lower limit of the TOC content in effective hydrocarbon source rocks (Fig. 5).

5. Results

5.1. Organic matter abundance, type and maturity

The results of the TOC, S_1, S_2, T_{max}, Ro, C, H, O element and maceral

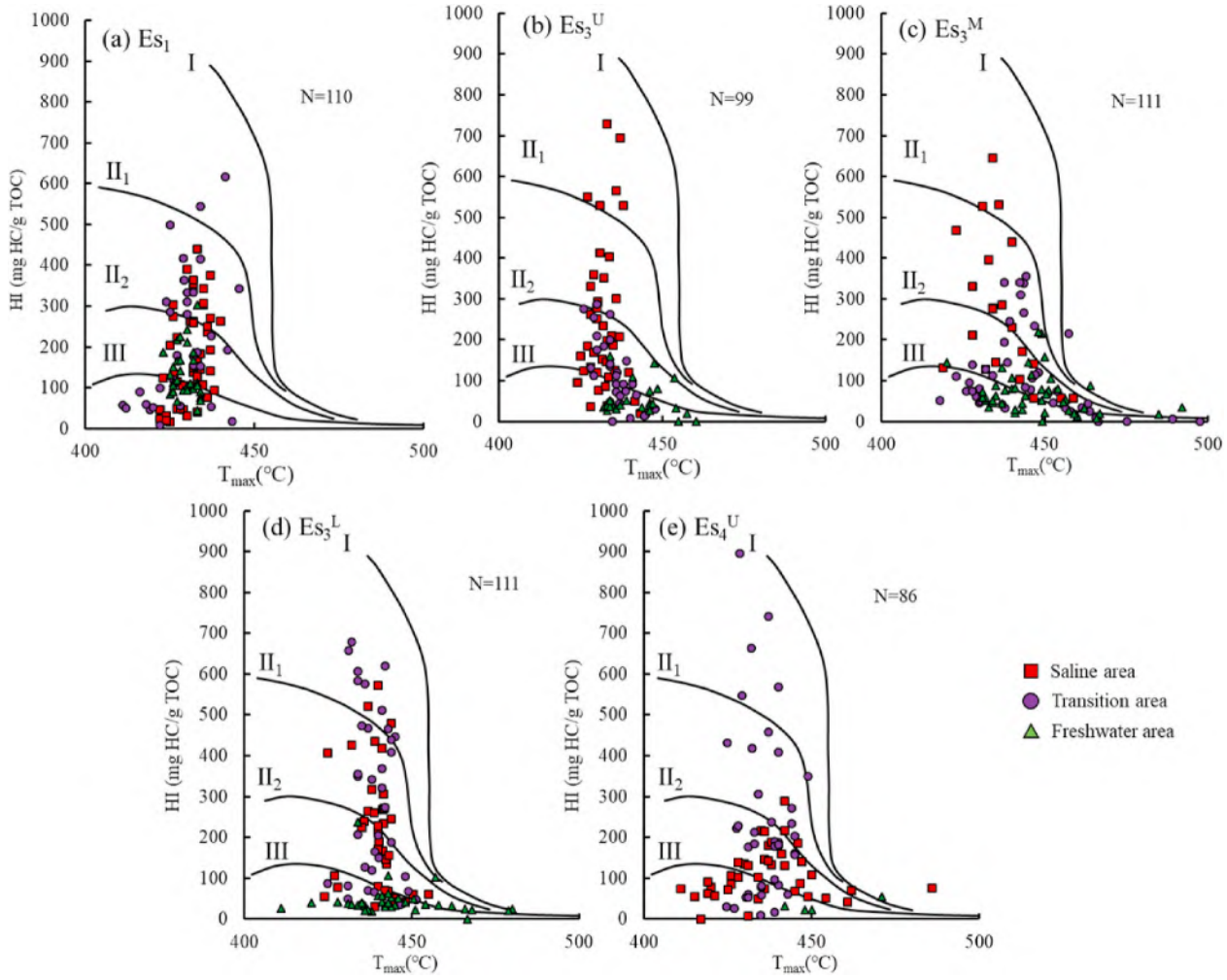

Fig. 11. Diagram of T_{max} and I_H of the Shahejie Formation source rock in the Dongpu Depression in different sedimentary environments: (a) first member of the Shahejie Formation (Es_1), (b) upper third submember of the Shahejie Formation (Es_3^U), (c) middle third submember of the Shahejie Formation (Es_3^M), (d) lower third submember of the Shahejie Formation (Es_3^L), and (e) upper fourth submember of the Shahejie Formation (Es_4^U). T_{max} = highest pyrolysis peak temperature; I_H = hydrocarbon index.

content are presented in Table 5. As a whole, the content of TOC varies between 0.02% and 5.7%, with an average value of 0.87%. The T_{max} value is 411–497 °C, and the mean value is 437.75 °C. The S_1 value ranges from 0 mg HC/g rock to 46.59 mg HC/g rock, with an average value of 1.19 mg HC/g rock. The S_2 value is 0–32.04 mg HC/g rock, and the average value is 2.27 mg HC/g rock. The HI value varies between 0 mg HC/g rock and 2152.93 mg HC/g rock, and the mean value is 177.96 mg HC/g rock.

5.2. Source rock distribution

According to the frequency diagram of the ratios of the source rock thickness to strata thickness in different sedimentary phases of each layer, the source rocks are mainly distributed in shore-shallow lake, delta front and saline lake facies (with mean values above 0.7, 0.62 and 0.54, respectively) (Table 2 and Fig. 6).

Mainly based on the strata thickness obtained by the logging data and the above ratios, the thickness of the source rocks in areas without enough wells or wells of sufficient depth was obtained, and then the plane distribution maps of the source rocks in each formation were predicted. The source rocks of Es_4^U and Es_3^L are widely distributed throughout the study area. The Es_4^U source rocks are mainly located in the Qianliyuan area with a maximum thickness of 600 m (1968 ft), while the Es_3^L thick source rocks are located in the center of the depression with a maximum thickness of 750 m (2460 ft) (Fig. 7A and B). The Es_3^M source rocks are also widely distributed in the center, and the maximum thickness is up to 800 m (2624 ft) (Fig. 7C). The Es_3^U source rocks are mainly located in the saline area, with a maximum thickness of 500 m (1640 ft) (Fig. 7D). The distribution area of Es_1 source rocks is similar to that of Es_3^U, with a maximum thickness of 300 m (984 ft) (Fig. 7E).

6. Discussion

6.1. Geochemical characteristics of different sedimentary environments

6.1.1. Organic matter abundance

The organic matter in rocks is the basis of hydrocarbon generation, and its amount can be used to effectively evaluate the hydrocarbon generation potential of the source rocks. The abundance of organic matter is often evaluated by the indicators of the TOC and hydrocarbon generation potential ($P_g = S_1+S_2$) (Peters, 1986; Tissot and Welte., 1984; Zhao et al., 2001; Wang et al., 2019; Si et al., 2020).

According to the evaluation criteria for organic matter abundance of lacustrine source rocks (Huang et al., 1984; Chen et al., 1997; Jia et al., 2016), the lacustrine source rocks can be divided into four categories based on TOC content: none (<0.4%), poor (0.4%–0.6%), fair (0.6%–1.0%) and good (>1.0%). The TOC content of the saline area ranges from 0.10% to 5.70%, with an average of 1.17%, and that of the

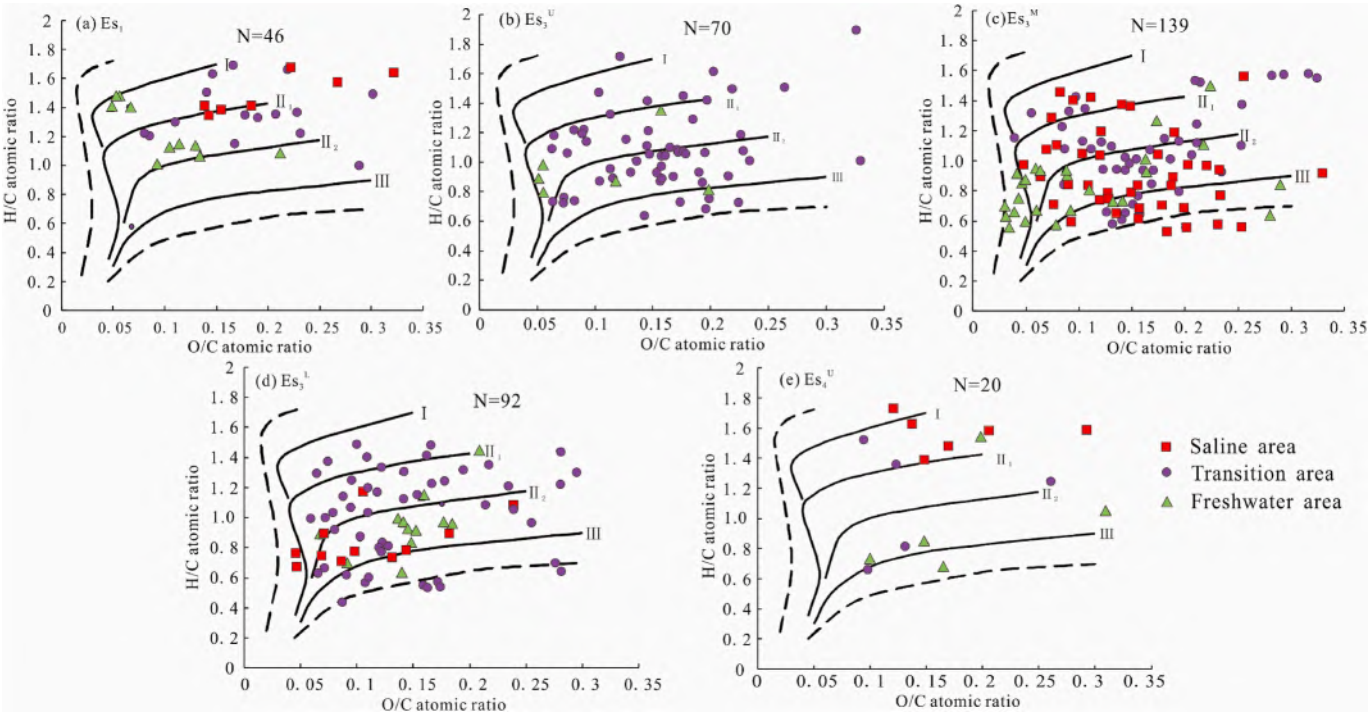

Fig. 12. Diagram of O/C and H/C atomic ratios of the Shahejie Formation source rock in the Dongpu Depression in different sedimentary environments: (a) first member of the Shahejie Formation (Es_1), (b) upper third submember of the Shahejie Formation (Es_3^U), (c) middle third submember of the Shahejie Formation (Es_3^M), (d) lower third submember of the Shahejie Formation (Es_3^L), and (e) upper fourth submember of the Shahejie Formation (Es_4^U).

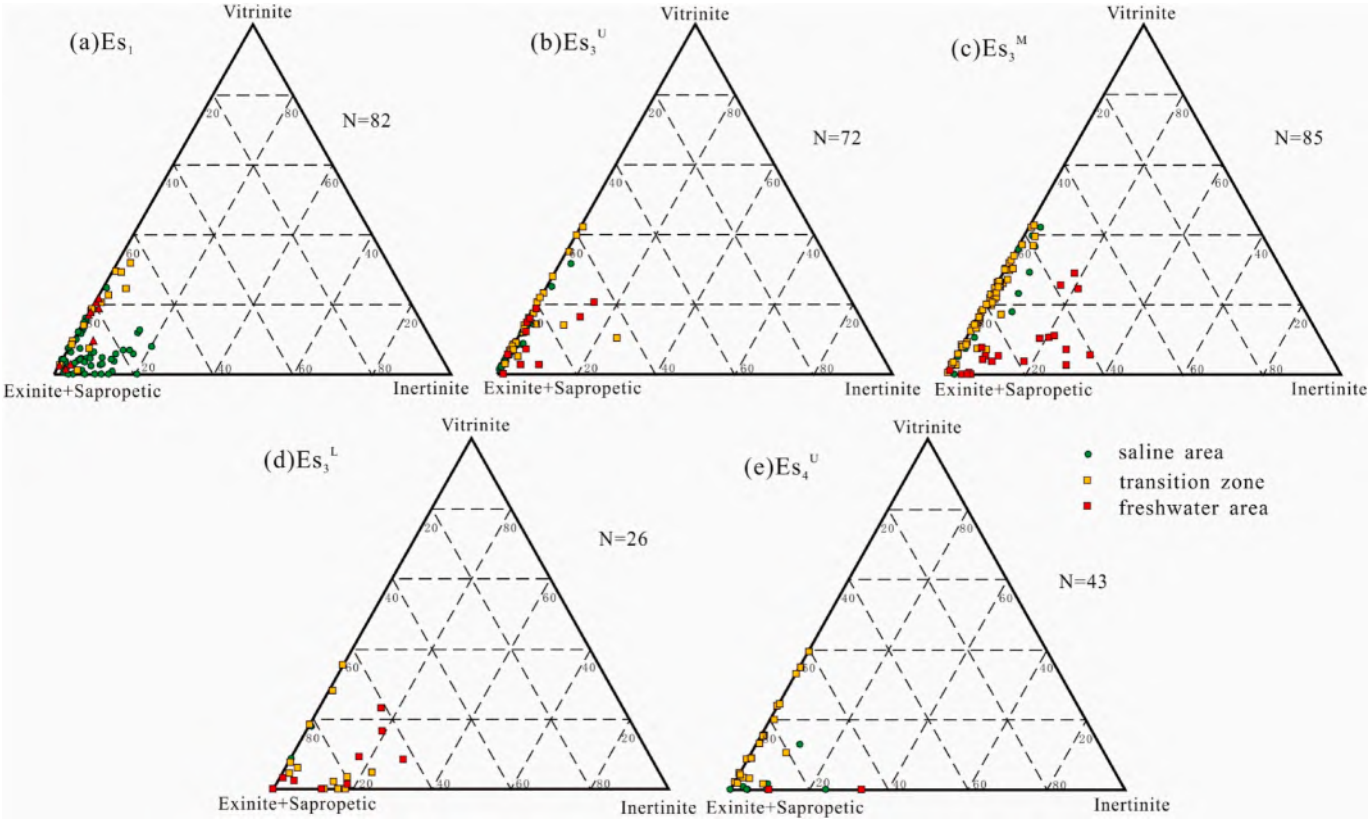

Fig. 13. Triangular diagram of organic matter macerals of the Shahejie Formation source rock in the Dongpu Depression in different sedimentary environments: (a) first member of the Shahejie Formation (Es_1), (b) upper third submember of the Shahejie Formation (Es_3^U), (c) middle third submember of the Shahejie Formation (Es_3^M), (d) lower third sub-member of the Shahejie Formation (Es_3^L), and (e) upper fourth sub-member of the Shahejie Formation (Es_4^U).

Table 3
Division of organic matter types by kerogen macerals.

Organic matter types	Type index (TI)
I	≥80
II_1	80–40
I_2	40–0
III	< 0

transition area is between 0.02% and 5.56%, with an average of 0.84%. The frequency distributions of TOC content in these two areas are relatively uniform, and the TOC values of 57% of the samples are more than 0.6% (Table 5). However, there are obvious differences in the two areas of the Es_3^U. Compared with the high TOC values in the saline area, those in the transition area are all less than 1%, and only 0.04% of samples have values exceeding 0.6%. The TOC values of the freshwater area are between 0.09% and 2.35%, with an average of 0.44%. Moreover, the TOC values are mostly lower than 1% in each formation, and approximately 80% of samples have values less than 0.6% (Table 5). The source rocks in the saline and transition areas have high abundance of organic matter and good hydrocarbon production foundation (Fig. 8).

The P_g values are 0.06%–54.53% in the saline area (mean value: 5.92%), 0.01%–25.57% in the transition area (mean value: 2.94%), and 0.03%–7.33% in the freshwater area (mean value: 0.56%) (Table 5). As shown in Fig. 9, the plots of TOC versus P_g are introduced to identify the quality of the source rocks. Most of the samples are fair to good source rocks in the saline and transition areas, but there are few samples of fair to good source rocks in the freshwater area. Generally, the source rocks in the saline and transition areas are fair to good, with high hydrocarbon generation potential. The quality of the source rocks in the freshwater area is poor, although some source rocks still have certain hydrocarbon generation potential (Figs. 8 and 9).

Generally, compared with the lower TOC in the freshwater area, the TOC is higher in the northern saline and transition areas, where fair to good source rocks are mainly developed. The TOC content varies in different formations, and the areas with high abundance of organic matter in each formation are mostly located in the saline and transition areas in the north (Fig. 10).

6.1.2. Organic matter type

The type of organic matter can be determined by pyrolysis data, elemental analysis data and maceral analysis data (Peters and Cassa, 1994; Hunt, 1996; Espitalie et al., 1986; Van Krevelen, 1961). Organic matter (kerogen) is usually classified into type I, type II_1, type II_2 and type III (Tissot and Welte, 1984; Mukhopadhyay et al., 1995; Guo et al.,

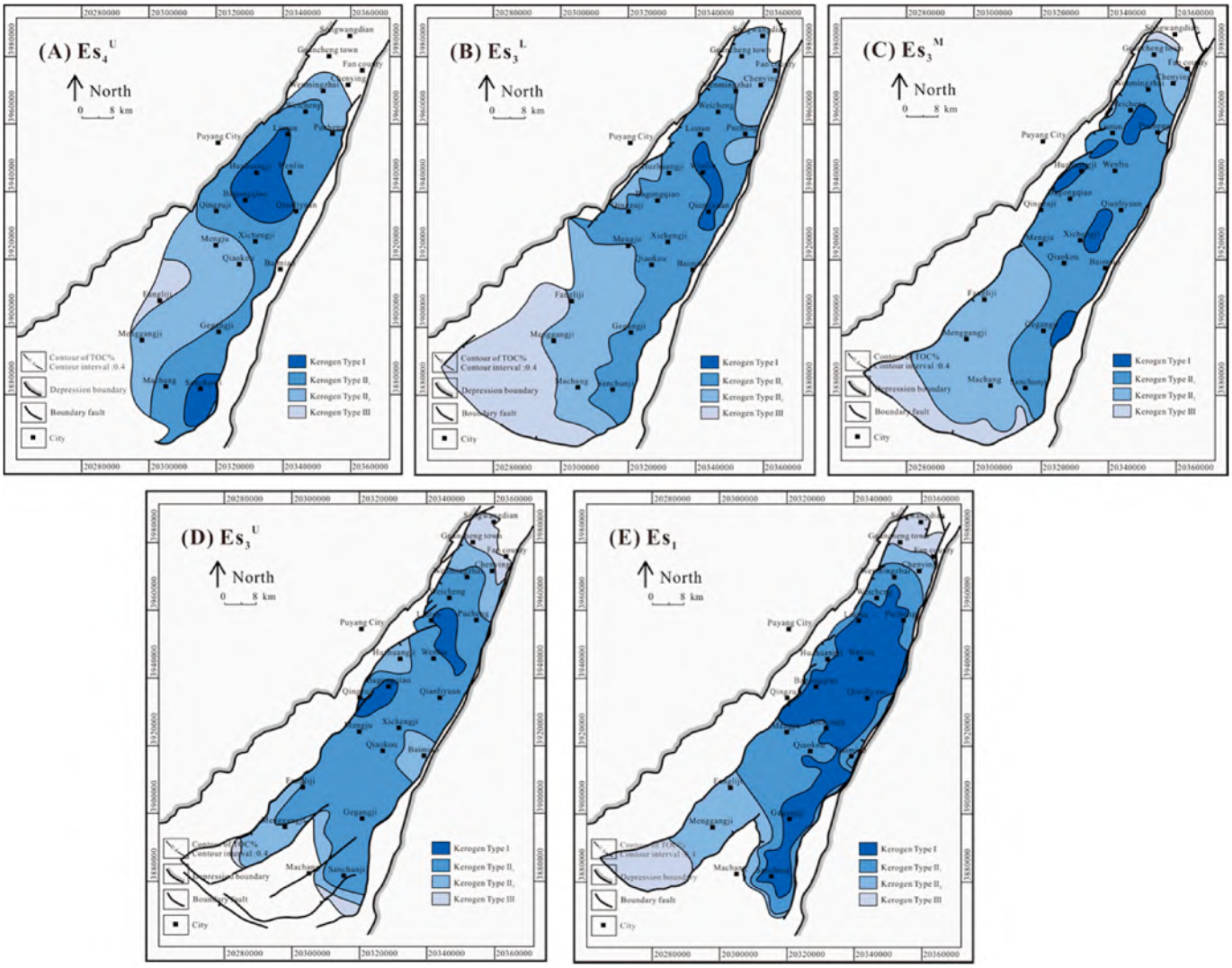

Fig. 14. Areal distribution chart of organic types for the Shahejie Formation source rock in the Dongpu Depression: (A) first member of the Shahejie Formation (Es_1), (B) upper third submember of the Shahejie Formation (Es_3^U), (C) middle third submember of the Shahejie Formation (Es_3^M), (D) lower third submember of the Shahejie Formation (Es_3^L), and (E) upper fourth submember of the Shahejie Formation (Es_4^U).

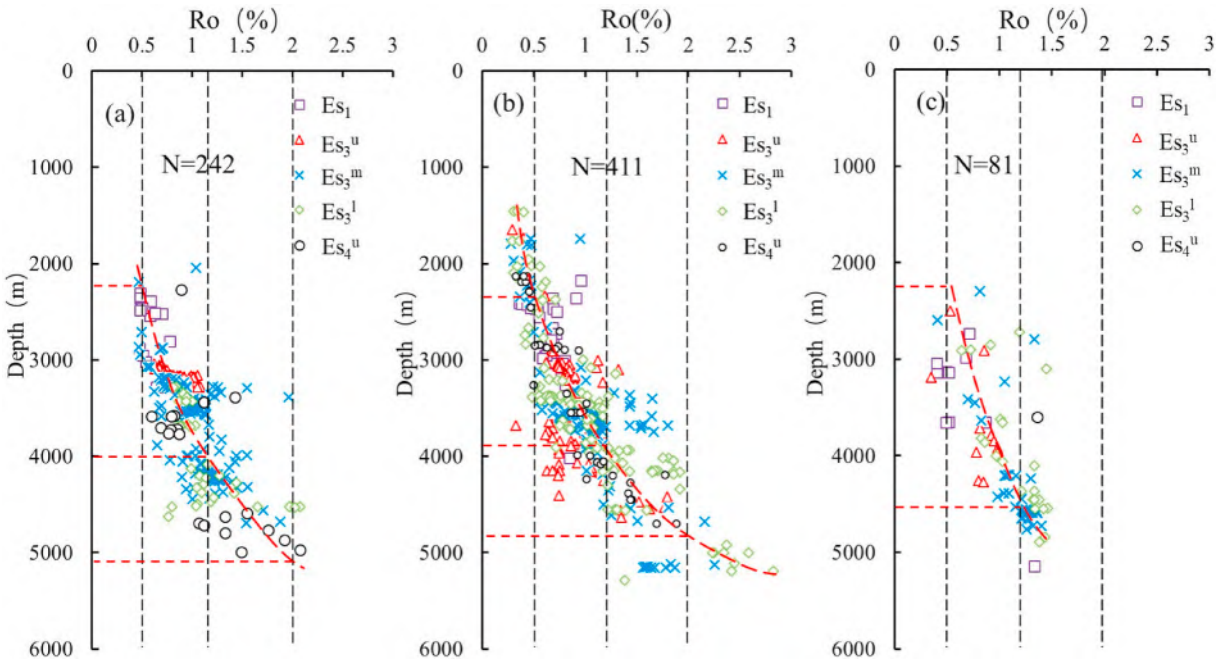

Fig. 15. Thermal evolution of source rocks in different sedimentary environments in the Dongpu Depression: (a) saline area, (b) transition area, and (c) freshwater area.

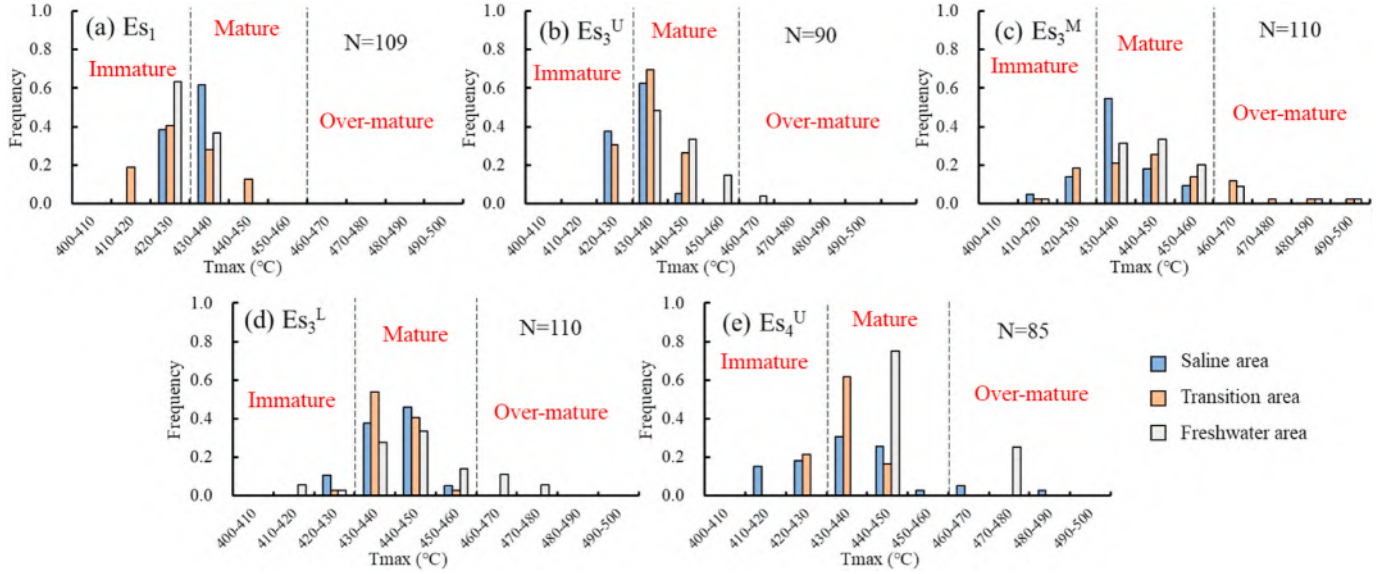

Fig. 16. Areal distribution of modern degree of thermal evolution of the Shahejie Formation source rocks in the Dongpu Depression: (a) first member of the Shahejie Formation (Es_1), (b) upper third submember of the Shahejie Formation (Es_3^U), (c) middle third submember of the Shahejie Formation (Es_3^M), (d) lower third submember of the Shahejie Formation (Es_3^L), and (e) upper fourth submember of the Shahejie Formation (Es_4^U).

2014). As shown in Fig. 11, most of the samples in the saline and transition areas for each formation are type II_1 and type II_2 kerogen and contain a small amount of type III kerogen; all the samples in the freshwater area are type III kerogen. The organic matter types of Es_4^U source rocks are poor, with more type III kerogen. Es_3^L and Es_3^M source rocks are mainly type II_1 and type II_2 kerogen in the saline and transition areas but type III kerogen in the freshwater area. Es_3^U and Es_1 source rocks are mainly type II_1 and type II_2 kerogen in the saline and transition areas. With regard to the freshwater area, the organic matter is dominated by type II_2 and type III kerogen. (Fig. 11).

The types of organic matter determined by pyrolysis data are sometimes affected by the thermal evolution degree of the source rock (Luo et al., 2011). To ensure the accuracy of the results, element analysis data can also be used to determine the types of organic matter (Yang et al., 1981; Damste et al., 1992). Overall, the results of organic matter types are consistent with those obtained with pyrolysis data. However, the organic matter types of Es_4^U source rocks in the saline and transition areas are mainly type I and type II_1 kerogen, which is different from the results obtained by pyrolysis data. The reason may be that the buried depth of the Es_4^U is greater than 4000 m, which can affect the accuracy of the T_{max} value (Fig. 12).

The hydrocarbon generation potential and type of organic matter can also be determined according to the results of maceral analysis, (Chen et al., 2007; Boussafir et al., 1995; Tu et al., 1998; Caplan et al., 1999).

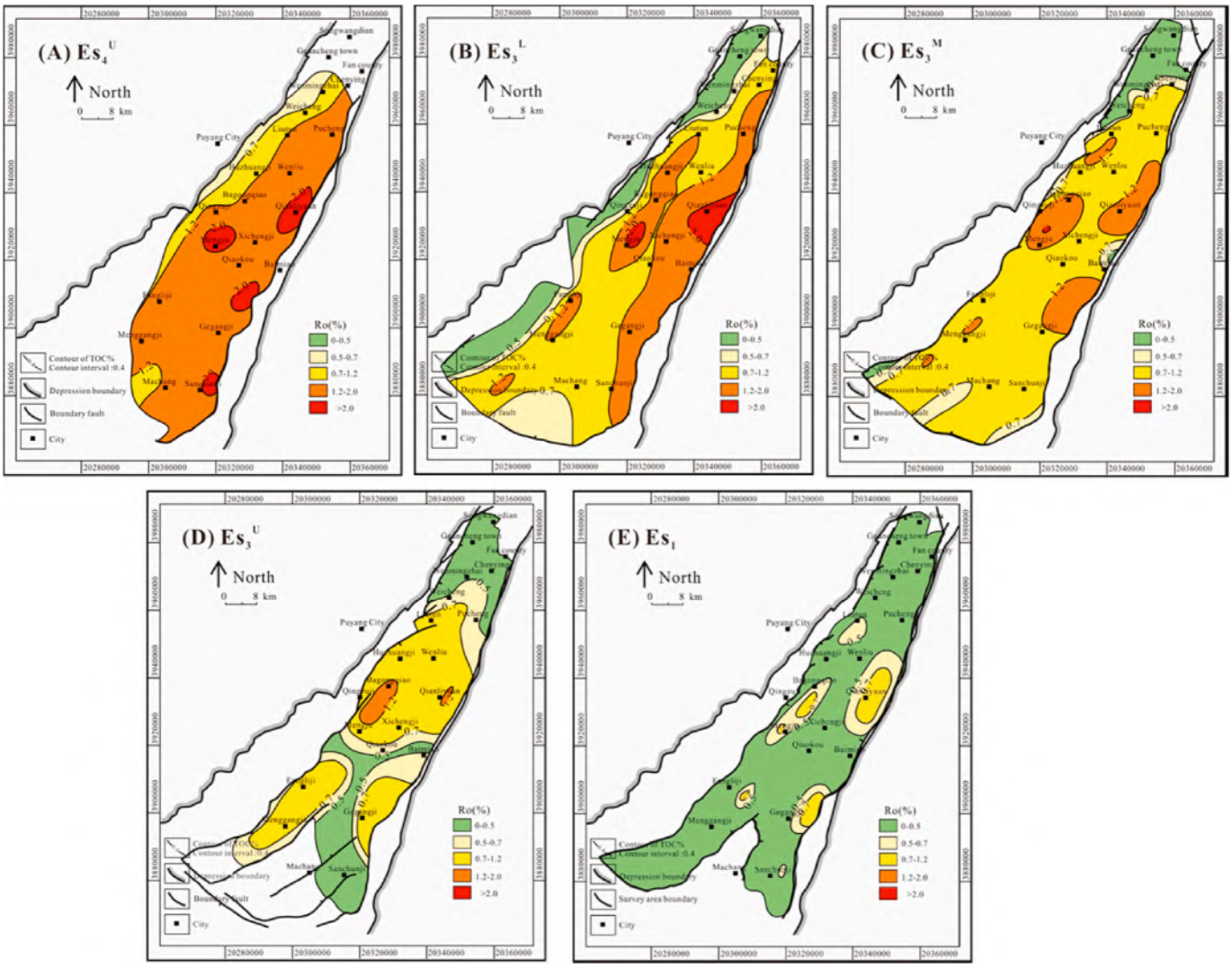

Fig. 17. Areal distribution of modern degree of thermal evolution of the Shahejie Formation source rocks in the Dongpu Depression: (A) first member of the Shahejie Formation (Es_1), (B) upper third submember of the Shahejie Formation (Es_3^U), (C) middle third submember of the Shahejie Formation (Es_3^M), (D) lower third submember of the Shahejie Formation (Es_3^L), and (E) upper fourth submember of the Shahejie Formation (Es_4^U).

The sums of sapropelinite and exinite of the samples from the saline area of each formation are higher than 80%, and only a small amount of vitrinite is found in Es_3^U and Es_3^M source rocks. This condition indicates that the source rocks in the saline area have good hydrocarbon generation potential (Jia et al., 2013). The sums of sapropelinite and exinite of the samples from each formation in the transition area are approximately 60%, the vitrinite content is approximately 40%, and the inertinite content is low, indicating that the hydrocarbon generation potential in the transition area is lower than that in the saline area. The contents of sapropelinite and exinite of the samples in the freshwater area are the lowest, which indicates that the organic parent material of the source rocks in the freshwater area is more complex and that their hydrocarbon generation ability is the worst (Fig. 13).

To study the plane distribution of organic matter types in each formation in detail, maceral data were used to calculate the type index (TI), which can obtain the distribution characteristics of organic matter types (Cao et al., 1985; Shen et al., 2013). The calculation formula of TI is as follows:

$$TI = 100 \times A + 50 \times B - 75 \times C - 100 \times D$$

where A is the content of sapropelinite, B is the content of exinite, C is the content of vitrinite, and D is the content of inertinite, unit = %. The TI classified according to the classification standard of organic matter is shown in Table 3.

The distribution of organic matter types differs in each formation, but the source rocks that are generally close to the north of the Dongpu Depression are dominated by type I and type II kerogen. Specifically, the Es_4^U source rocks are mainly developed type I and type II_1 kerogen in the northern saline and transition areas, Es_3^M and Es_3^L source rocks are mainly developed type II_1 and type II_2 kerogen in the northern areas near gypsum formations, Es_3^U and Es_1 source rocks are mainly type I and II_1 in the whole depression, and the kerogen types in the south are mainly type II_2 and III in each formation (Fig. 14).

In summary, the kerogen types in the northern saline and transition areas of each formation are mainly type I and II, which are superior to the type III found in the southern freshwater area. For each formation, the kerogen types of Es_1 and Es_3 source rocks are mainly type II and III, and those of Es_4^U source rocks are mainly type III.

6.1.3. Organic matter thermal maturity

The vitrinite reflectivity (Ro) and the maximum peak temperature of pyrolysis (T_{max}) are usually used to evaluate the degree of thermal evolution of organic matter (Peters et al., 2005; Tissot and Welte, 1980; Tissot, 1987).

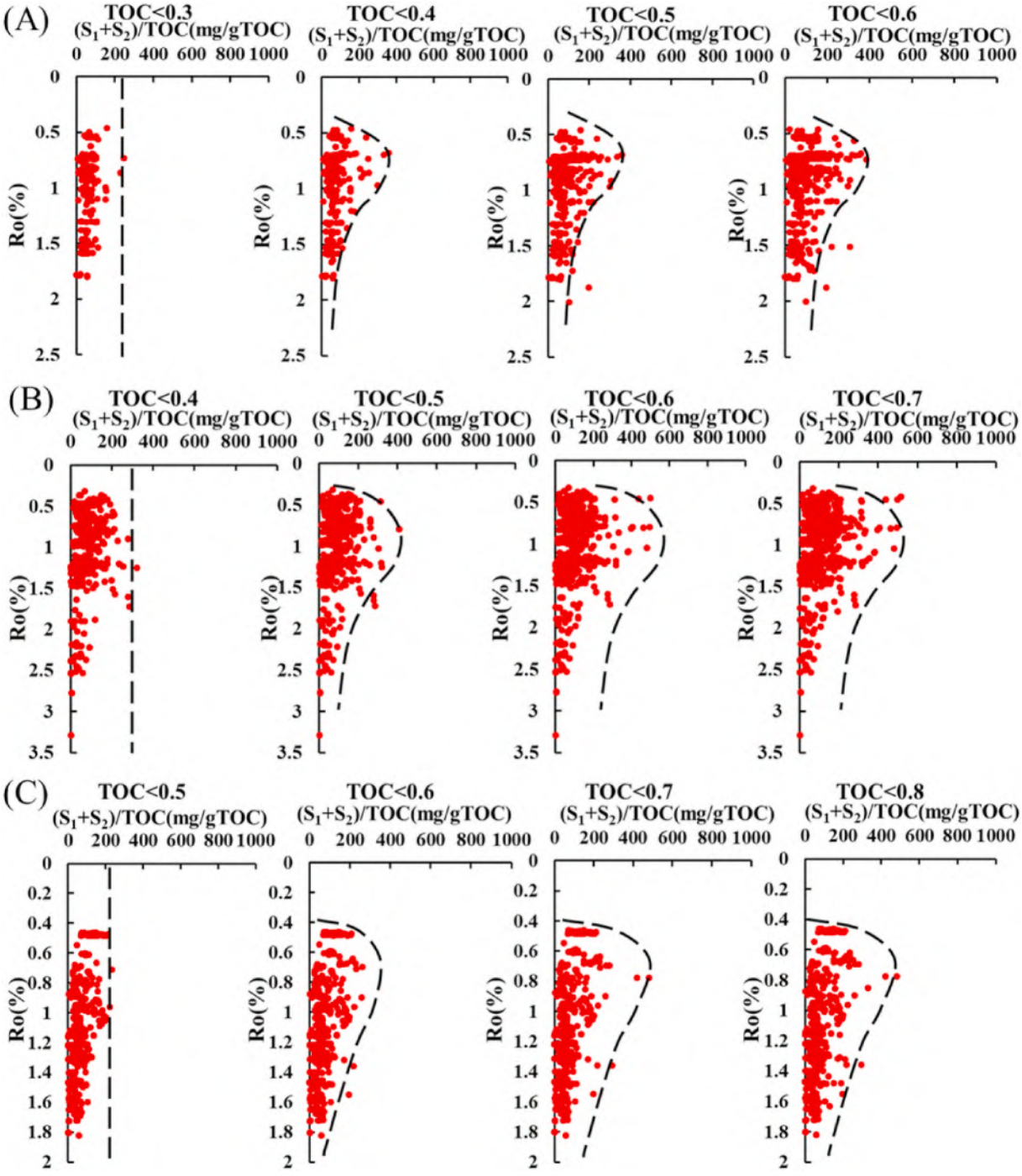

Fig. 18. Hydrocarbon generation potential index profiles of different sedimentary environments in the Dongpu Depression: (A) saline area, (B) transition area, and (C) freshwater area.

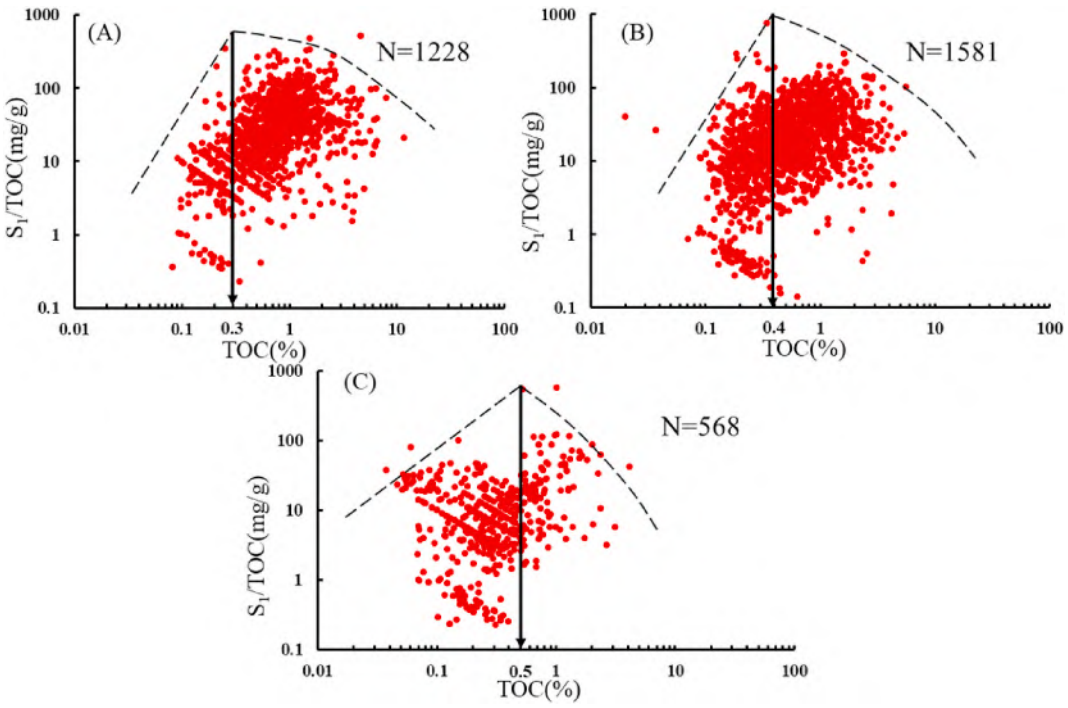

Fig. 19. Scatter plots of TOC and pyrolysis S_1 in different sedimentary environments of the Shahejie Formation in the Dongpu Depression: (A) saline area, (B) transition area, and (C) freshwater area.

Table 4
Identification of effective source rocks via several methods.

Method	Lower limit of effective source rocks in saline area	Lower limit of effective source rocks in transition zone	Lower limit of effective source rocks in freshwater area
Hydrocarbon potential method	0.30%	0.40%	0.50%
S_1 and TOC method	0.30%	0.40%	0.50%

The maximum Ro value reaches 2.07% in the saline area, 2.85% in the transition area, and 1.46% in the freshwater area. The source rocks enter the oil generation window at a depth of 2200–4000 m for the saline area and 2300–3920 m for the transition area. When the depth exceeds 4000 m (13,120 ft), these source rocks reach the stage of pyrolysis gas generation. The Ro values of the source rocks in the freshwater area are mainly 0.50%–1.50%, which indicates that the source rocks are mainly in the oil-generating stage and are just beginning to generate gas (Fig. 15). The thermal evolution degree of deeper source rocks needs further analysis and research.

The thermal evolution degree of organic matter is different in each formation, and that in different sedimentary environments of the same formation is also different. According to the T_{max} data, all of the Es_1 samples and 99% of the Es_3^U samples are in the immature-mature stage, 75% of the Es_3^M samples and 87% of the Es_3^L samples are in the mature stage, and 95% of the Es_4^U samples are in the immature-mature stage (Fig. 16). The above results indicate that most of the source rocks are in the immature-mature stage, and the Es_3^M and Es_3^L source rocks are mostly mature.

Based on the correlation between Ro data and depth, the plane distribution of the thermal evolution degree of organic matter in the Dongpu Depression was predicted (Fig. 17). The results show that the thermal evolution of Es_1 source rocks is low, with a maximum Ro value of 0.70%. In addition, the source rocks in most areas are in the immature stage, and only small parts of those in the Qinliyuan, Qingzuji and Gegangji areas are in the mature stage. The evolution degree of the Es_3^U source rocks is relatively high, and the Ro values of the most areas reach 0.70%, showing that the source rocks in the northern area, the Gegangji area and Fangliji area in the south have reached the mature stage. The source rocks of Es_3^M have reached the mature stage in both the north and the south areas (Qianliyuan and Qingzuji). The Es_3^L source rocks have reached the mature stage in the east and the highly mature stage in the Qianliyuan area, and only those in a small part of the western areas remain at the immature stage. Es_4^U source rocks of most areas have reached the highly mature stage, such as in the Bagongqiao and Qingzuji areas.

6.2. *Effective source rock characteristics of different sedimentary environments*

6.2.1. *Lower limit of effective source rocks*

Based on the hydrocarbon generation potential method, the results show that the lower limit of effective source rocks is TOC>0.3% in the saline area, TOC>0.4% in the transition area, and TOC>0.5% in the freshwater area (Fig. 18).

According to the contents of S_1 and TOC, the hydrocarbon in the source rock after filling the pores of the rocks will be expelled from the source rock. Fig. 19 shows that the lower limit of the TOC content of the Dongpu Depression is 0.3% in the saline area, 0.4% in the transition area, and 0.5% in the freshwater area.

6.2.2. *Difference between the two methods*

The results from the two methods on the lower limit of the TOC content for effective source rocks show that the lower limit is lower in the saline area, higher in the transition area, and the highest in the freshwater area (Table 4). K_2qn_1 (first member of Qingshakou Formation) source rocks in the Songliao Basin developed in a typical non-saline lacustrine sedimentary environment with a large area of thick black shale, and the lower limit of its effective source rocks is TOC>0.4% (Lei et al., 2016). Similarly, the lower limit of K_1c (Chijinbu Formation) effective source rocks in Jiuquan Basin is TOC>0.6% (Gao et al., 2012).

Table 5
Geochemical data of different sedimentary environments of the Shahejie Formation in the Dongpu Depression.

Fm.	D. E	TOC (%)	T_{max} (°C)	S_1 (mg/g)	S_2 (mg/g)	HI (mg/g)	H/C	O/C	Inertinite (%)	Sapropetic (%)	Exinite (%)	Vitrinite (%)
Es_1	S	0.26–1.8	422–440	0.01–1.97	0.06–7.31	16.34–440.36	1.35–3.14	0.14–2.95	0.3–21.01	2.35–100	1.68–85.57	0.6–24.64
		0.81	431.11	0.51	1.87	183.6	1.8	0.65	7.49	61.22	29.2	7.07
	T	0.13–3.82	411–445.4	0.01–1.71	0.01–15.91	7.6–617.01	0.58–1.73	0.07–0.59	0.26–5.86	1.41–89.78	3.87–85.76	1.1–31.71
		1.06	428.77	0.28	3.49	219.53	1.34	0.22	2.59	34.62	47.21	15.93
	F	0.22–0.9	423–434	0.02–0.11	0.13–2.73	44.83–303.73	1.00–1.47	0.05–0.21	0.26–4.94	2.69–89.94	6.32–77.18	1.72–21.79
		0.51	429.3	0.06	0.76	135.78	1.23	0.1	1.73	43.4	42.66	12.6
Es_3^U	S	0.18–5.7	424–443.2	0–5.53	0.1–22.98	19.2–1405.09	–	–	0.28–3.02	0.96–96.69	0.28–89.67	1.34–31.59
		0.98	432.06	0.66	3.48	300.98	–	–	0.84	59.05	32.09	8.27
	T	0.13–0.64	426–447.7	0–2.58	0–1.57	0.8–287.5	0.64–1.90	0.06–0.94	0.27–25.21	1.58–85.1	6.95–81.17	2.97–41.87
		0.36	435.62	0.28	0.5	119.24	1.11	0.19	2.95	24.75	57.42	15.86
	F	0.1–0.77	432–460.3	0–0.29	0–1.11	0.52–159.09	0.79–1.36	0.05–0.47	0.28–14.25	23.22–98.48	3.88–60.68	2.72–20.47
		0.27	442.12	0.03	0.16	50.81	0.93	0.16	4.87	60.45	27.01	11.63
Es_3^M	S	0.1–4.45	419–454.8	0–2.69	0.06–36.04	56.78–2152.93	0.53–1.56	0.05–0.40	0.32–7.94	2.87–100	0.32–66.67	5.11–41.85
		1	436.79	0.69	5.48	352.8	0.93	0.16	3.56	58.96	19.2	23.9
	T	0.02–5.56	418–497.4	0–5.78	0–19.79	0.27–355.92	0.58–3.64	0.04–2.33	0.26–6.72	0.6–96.23	0.94–86.26	0.59–42.55
		0.74	445.8	0.5	1.43	115.05	1.28	0.31	1.22	28.19	50.88	20.87
	F	0.13–2.35	420–492	0–5.88	0–5.05	0.85–219.75	0.54–3.05	0.03–2.33	0.56–33.72	16.51–99.37	0.31–41.63	0.62–28.97
		0.56	447.31	0.31	0.55	68.1	1.08	0.33	13.76	71.43	9.02	9.27
Es_3^L	S	0.14–4.7	424–455	0.01–3.47	0.08–19.63	29.31–571.59	0.68–2.05	0.05–1.16	0.31–0.66	10.2–11.95	71.38–79.25	8.49–17.76
		1.13	439.69	0.89	3.57	217.05	1.06	0.27	0.49	11.08	75.32	13.13
	T	0.1–4.27	425–451.2	0–1.19	0.04–24.58	35.66–679.36	0.44–1.71	0.06–1.28	0.58–22.59	0.65–93.75	1.43–80.97	1.91–35.24
		1.17	438.89	0.38	4.96	291.64	1.02	0.19	10.83	56.07	31.5	12.15
	F	0.09–1.56	411–480	0–1.11	0–1.9	0.43–237.5	0.63–3.55	0.07–4.18	0.98–28.62	1.58–96.77	2.11–87.73	1.17–22.89
		0.39	445.17	0.07	0.23	44.19	1.2	0.53	14.53	60.1	45	9.02
Es_4^U	S	0.16–5.69	411–486	0.01–46.59	0–7.94	0–288.06	1.39–1.73	0.12–0.41	2.99–24.32	43.54–89.91	0.63–32.41	0.6–12.66
		1.97	436.45	11.03	2.33	110.69	1.58	0.21	8.76	74.13	15.27	4.91
	T	0.08–3.34	424.5–449	0.01–0.93	0.04–22.16	10.15–1517.01	0.66–1.53	0.09–0.26	0.22–8.96	1.87–89.03	1.25–89.57	1.54–39.15
		0.81	435.6	0.2	2.53	298.98	1.12	0.14	1.54	53.38	31.3	13.92
	F	0.11–0.19	442–471	0.01–0.02	0.03–0.06	22.22–54.55	0.67–1.55	0.10–0.31	9.84–33.33	66.67–88.52	1.64	0
		0.15	452.75	0.01	0.05	32.86	0.97	0.18	21.59	77.6	1.64	0

Note:

The results describing the above-mentioned non-saline formation are similar to those for the transition and freshwater areas in the Dongpu Depression. Thus far, there is no definitive research result on the lower limit of effective source rocks of lacustrine saline formations. Moreover, the mechanisms involved in the difference of lower limits of effective hydrocarbon source rocks in different sedimentary environments need to be further studied.

6.2.3. Distribution of effective source rocks

According to the lower limit of effective source rocks in different sedimentary environments, plane distribution maps of five formations effective source rocks (Es_1, Es_3^U, Es_3^M, Es_3^L and Es_4^U) were obtained (Fig. 20).

The effective source rocks are unevenly distributed in the Dongpu Depression. The Es_4^U source rocks are buried deeper, and the thickness of the source rocks is mainly 100–250 m (328–820 ft). The main sedimentary center is located in the Wenliu area and Qianliyuan area at a maximum thickness of 279 m (915.12 ft) (Fig. 20A). The Es_3^L source rocks are also deeply buried and have good quality; therefore, the effective source rocks are distributed throughout the depression, with a thickness of 200–400 m (656–1312 ft), and the main sedimentary center is located near the Liutun area and the Gegangjig area, at a maximum thickness of 491 m (1610.48 ft) (Fig. 20B). In the south and surrounding parts, the distribution of effective source rocks in Es_3^U is relatively thin. Compared with other formations, the thickness of the effective source rocks in Es_3^M is the thickest, at 200–500 m (656–1640 ft), and the distribution range is relatively wide, covering almost the entire depression. The effective source rocks in the northern areas, Liutun area, Qianliyuan area, Qingzuji area and Gegangji area, are relatively thick, with a maximum of 630 m (2066.40 ft), and only the northern part and the southern edge of the depression have a thin distribution of effective source rocks (Fig. 20C and D). The effective source rocks in Es_3^U are in the Qianliyuan area, Mengju area and Bagongqiao area, with the thickness ranging from 100 to 200 m (328–656 ft) and a maximum thickness of 320 m (1049.60 ft). The Es_1 effective source rocks are mainly distributed in the Mengju area and Qianliyuan area, with a maximum thickness of 351 m (1151.28 ft), and there are no effective source rocks in the south (Fig. 20E).

6.3. Hydrocarbon expulsion characteristics of different sedimentary environments

6.3.1. Hydrocarbon expulsion model

The hydrocarbon expulsion models of effective source rocks in different sedimentary environments in the Dongpu Depression were established using the hydrocarbon generation potential method.

The hydrocarbon expulsion thresholds of effective source rocks in the saline area, transition area and freshwater area are 0.65%, 0.68% and 0.7%, respectively. Different environments have different hydrocarbon expulsion ratios. Specifically, the maximum hydrocarbon expulsion ratio is 439.45 mg/g in the saline area, 369.32 mg/g in the transition area, and 253.09 mg/g in the freshwater area. The reason for this difference is that high-salinity water is conducive to the enrichment of organic parent materials and the formation of a reductive environment, which provides a good basis for the preservation of organic matter (Hu et al., 2018). Therefore, the source rocks in the saline area have a good hydrocarbon generation capacity, which enables the sufficient generation of hydrocarbon to reach the critical saturation of residual hydrocarbon, followed by the expulsion of a large amount of hydrocarbon.

Based on observation and analysis, the hydrocarbon expulsion rate of organic matter in the saline, transition and freshwater areas showed a trend of initially increasing and then decreasing with increasing Ro. The hydrocarbon expulsion rate of the source rocks increases slowly and reaches a peak value of 59.6‰ in the saline area when the Ro value is 0.95%, increases slightly and reaches a peak value of 55.33‰ in the transition area when the Ro value is 0.85% and increases quickly and reaches a peak value of 74.25‰ in the freshwater area when the Ro

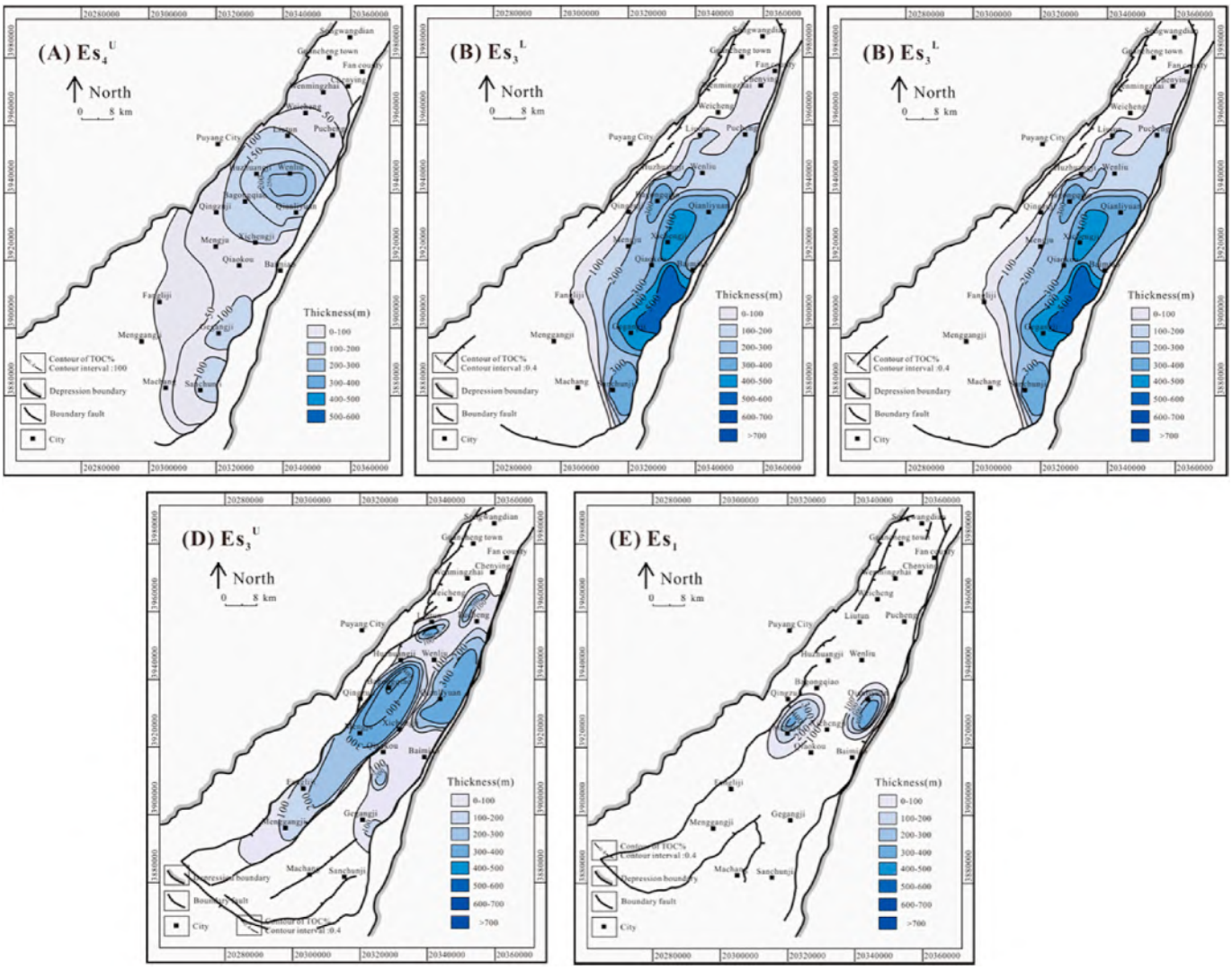

Fig. 20. Areal distribution chart of effective source rocks for the Shahejie Formation in the Dongpu Depression: (A) first member of the Shahejie Formation (Es_1), (B) upper third submember of the Shahejie Formation (Es_3^U), (C) middle third submember of the Shahejie Formation (Es_3^M), (D) lower third submember of the Shahejie Formation (Es_3^L), and (E) upper fourth submember of the Shahejie Formation (Es_4^U).

value is 0.82%.

With increasing Ro, the hydrocarbon expulsion efficiency increases gradually in all three environments. Clearly, the rate of increase in the saline area is relatively slow, that in the transition area is faster, and that in the freshwater area is the fastest, with maximum hydrocarbon expulsion efficiencies of 85.32%, 86.42% and 85.5%, respectively (Fig. 21). The mechanism underlying the highest hydrocarbon expulsion rate and efficiency in the saline area but the lowest in the freshwater area needs to be further studied.

6.3.2. Hydrocarbon expulsion history and quantity

6.3.2.1. Upper fourth submember of the Shahejie Formation. The Es_4^U source rock began to discharge hydrocarbon at approximately 45–33 Ma; the hydrocarbon expulsion center was located in the Qianliyuan area, and the hydrocarbon expulsion area occurred across a large are in both the north and south. The maximum hydrocarbon expulsion intensity was 0.03×10^8 t/km^2 (0.22×10^8 bbl/km^2) in the north, and the hydrocarbon expulsion amounts in the saline, transition and freshwater area were 2×10^8 t (14.60×10^8 bbl), 0.68×10^8 t (4.96×10^8 bbl), and 0.31×10^8 t (2.26×10^8 bbl), respectively. In the process of hydrocarbon expulsion from the Es_4^U source rocks, the area of hydrocarbon expulsion underwent few changes, and the center of hydrocarbon expulsion remained unchanged. Currently, the maximum hydrocarbon expulsion intensity is 0.07×10^8 t/km^2 (0.51×10^8 bbl/km^2). The amounts of cumulative hydrocarbon expulsion in the saline, transition and freshwater areas are 9.77×10^8 t (71.32×10^8 bbl), 3.58×10^8 t (26.13×10^8 bbl) and 2.59×10^8 t (18.91×10^8 bbl), respectively (Fig. 22).

6.3.2.2. Lower third submember of the Shahejie Formation. The Es_3^L source rocks began to discharge a small amount of hydrocarbon in the Qianliyuan area at the end of Es_3 (35 Ma). The hydrocarbon expulsion amounts in the saline, transition and freshwater area are 0.02×10^8 t (0.15×10^8 bbl), 0.85×10^8 t (6.21×10^8 bbl) and 0.06×10^8 t (0.44×10^8 bbl), respectively. During the Ed depositional period (33-17 Ma), the area of hydrocarbon expulsion was connected between the south and north, and the hydrocarbon expulsion center was located in the Qianliyuan area, Gegangji area and Mengju area. The maximum hydrocarbon expulsion intensity in the north was 0.02×10^8 t/km^2 (0.15×10^8 bbl/km^2), whereas the south had almost no hydrocarbon expulsion. Currently, the hydrocarbon expulsion center of the Es_3^L source rocks

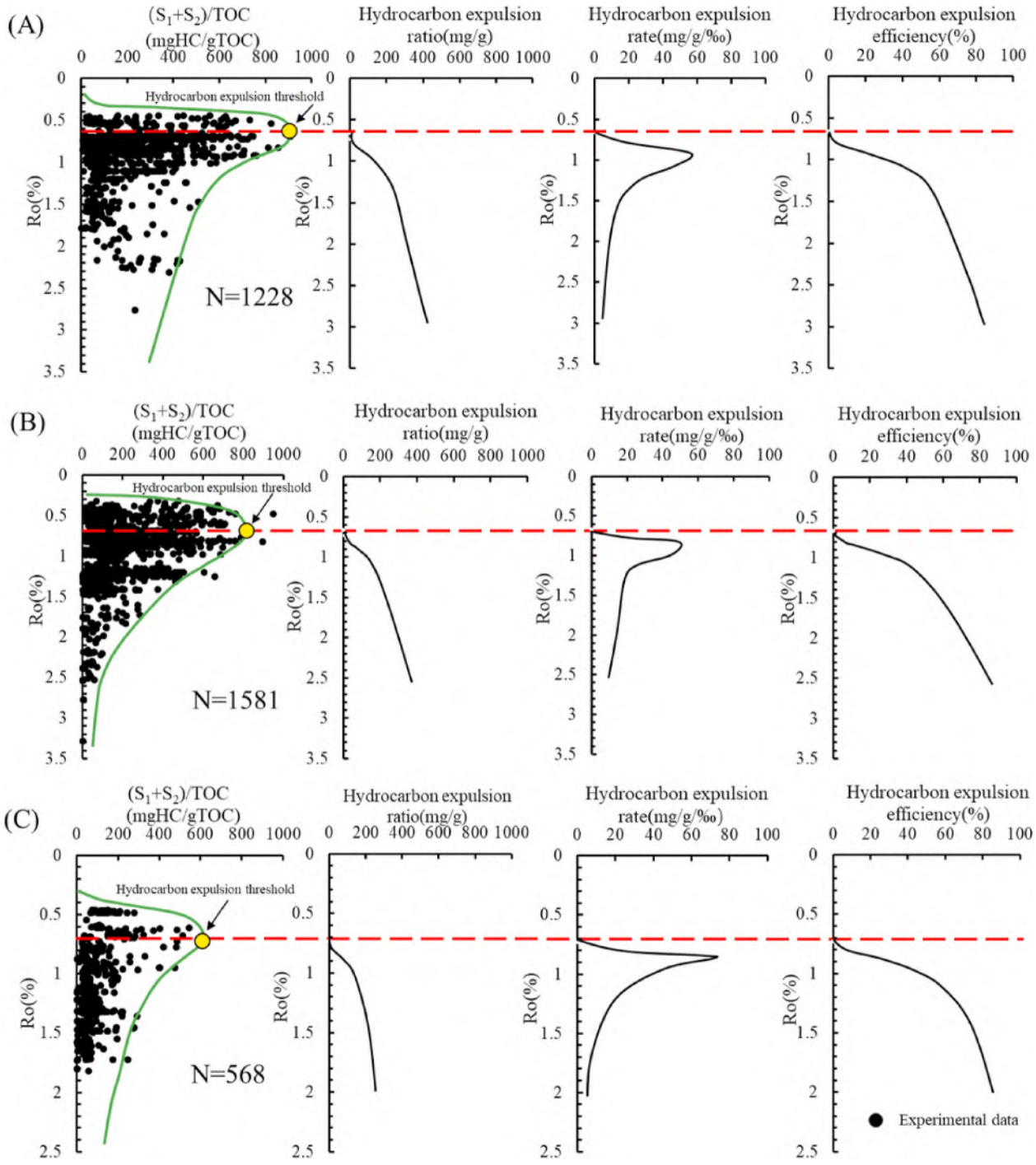

Fig. 21. Hydrocarbon generation and expulsion quantitative model in different sedimentary environments of the Shahejie Formation in the Dongpu Depression: (A) saline area, (B) transition area, and (C) freshwater area.

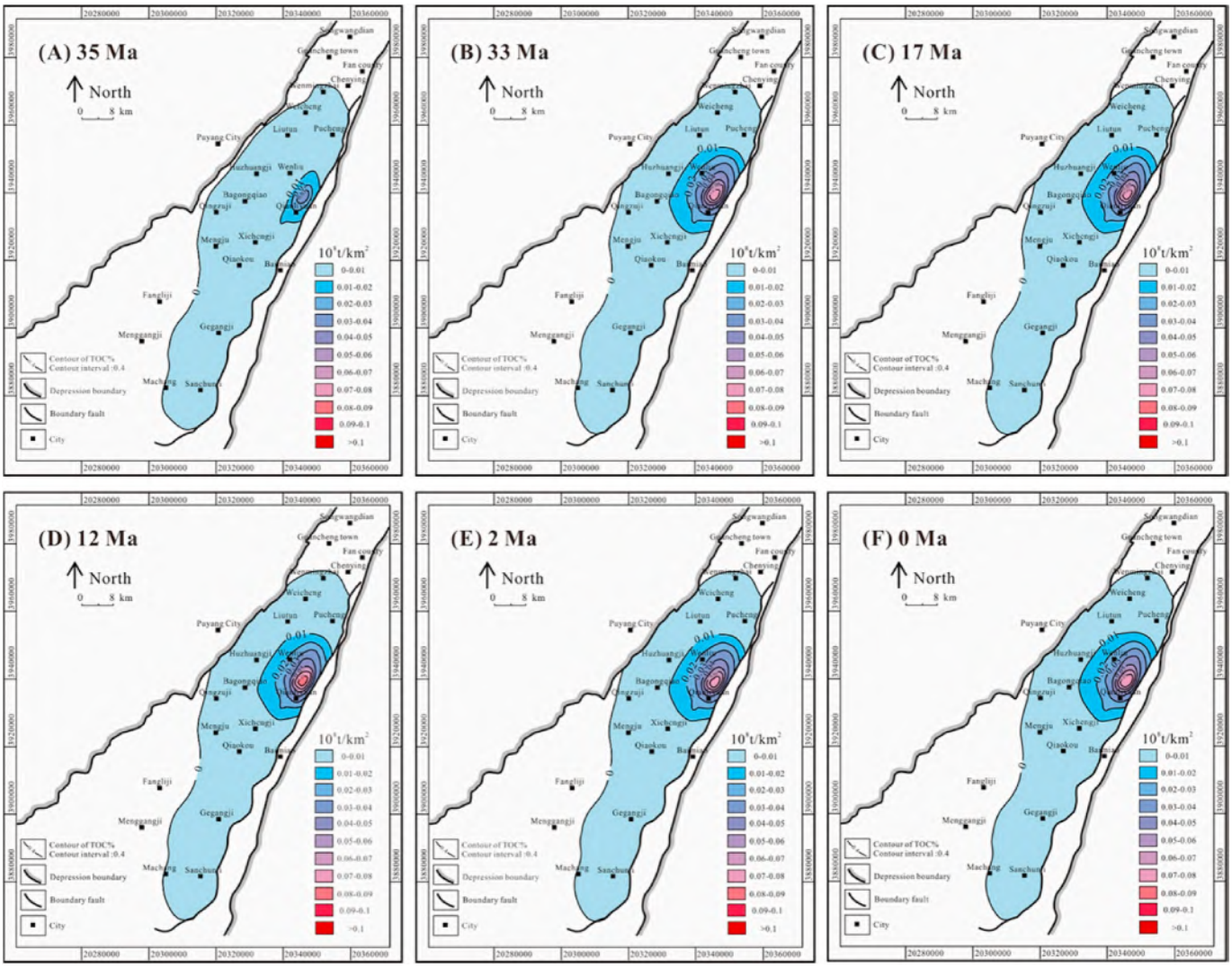

Fig. 22. Hydrocarbon expulsion intensity map of the effective source rocks of the first member of the Shahejie Formation in different periods: (A) 17 Ma, (B) 12 Ma, (C) 2 Ma and (D) modern.

remains unchanged. The maximum hydrocarbon expulsion intensity reached 0.07 × 10^8 t/km^2 (0.51 × 10^8 bbl/km^2). The amount of cumulative hydrocarbon expulsion in the saline, transition and freshwater areas was 4.00 × 10^8 t (29.20 × 10^8 bbl), 18.81 × 10^8 t (137.31 × 10^8 bbl) and 13.63 × 10^8 t (99.50 × 10^8 bbl), respectively (Fig. 23).

6.3.2.3. Middle third submember of the Shahejie Formation. The Es_3^M source rocks reached the hydrocarbon expulsion threshold at the end of Es_3 (35 Ma) with a very small amount of hydrocarbon expulsion. Hydrocarbon was not discharged in the south. The maximum hydrocarbon expulsion intensity in the north was 0.01 × 10^8 t/km^2 (0.07 × 10^8 bbl/km^2). The hydrocarbon expulsion intensity increased during the period from 33 to 17 Ma. There was a large amount of hydrocarbon expulsion in the Qianliyuan area, Gegangji area and Qingzuji area, and expulsion began in the Qiandugu area. Currently, the maximum of the hydrocarbon expulsion intensity is 0.10 × 10^8 t/km^2 (0.74 × 10^8 bbl/km^2) in the north. The amount of cumulative hydrocarbon expulsion in the saline, transition and freshwater area is 4.05 × 10^8 t (29.57 × 10^8 bbl), 14.79 × 10^8 t (107.97 × 10^8 bbl) and 7.78 × 10^8 t (56.80 × 10^8 bbl), respectively (Fig. 24).

6.3.2.4. Upper third submember of the Shahejie Formation. The Es_3^U source rocks reached the hydrocarbon expulsion threshold at the end of Es_1 (33 Ma), with a small scope of hydrocarbon expulsion and a small amount of hydrocarbon expulsion, which mainly occurred in the northern region. Specifically, the hydrocarbon expulsion amount in the saline area was 0.0005 × 10^8 t (0.004 × 10^8 bbl), that in the transition zone was 0.30 × 10^8 t (2.19 × 10^8 bbl), and hydrocarbon expulsion did not occur in the freshwater area. At the end of Ed deposition (33-17 Ma), the hydrocarbon expulsion area expanded; the hydrocarbon expulsion amounts in the saline area and transition area were 0.03 × 10^8 t (0.22 × 10^8 bbl) and 1.42 × 10^8 t (0.37 × 10^8 bbl), respectively, and the freshwater area just began to discharge hydrocarbons, at a hydrocarbon expulsion amount of 0.03 × 10^8 t (0.22 × 10^8 bbl). Currently, the maximum hydrocarbon expulsion intensity in the north has reached 0.04 × 10^8 t/km^2 (0.29 × 10^8 bbl/km^2), and that in the south is 0.01 × 10^8 t/km^2 (0.07 × 10^8 bbl/km^2). The amounts of cumulative hydrocarbon expulsion in the saline, transition and freshwater areas are 0.07 × 10^8 t (0.51 × 10^8 bbl), 3.57 × 10^8 t (26.06 × 10^8 bbl) and 0.12 × 10^8 t (0.88 × 10^8 bbl), respectively (Fig. 25).

6.3.2.5. First member of the Shahejie Formation. The Es_1 source rocks began to expel hydrocarbons during the depositional period of the Dongying Formation (33-17 Ma). During this period, only a small amount of hydrocarbon was discharged from the northern region with a low hydrocarbon expulsion intensity (no more than 0.01 × 10^8 t/km^2

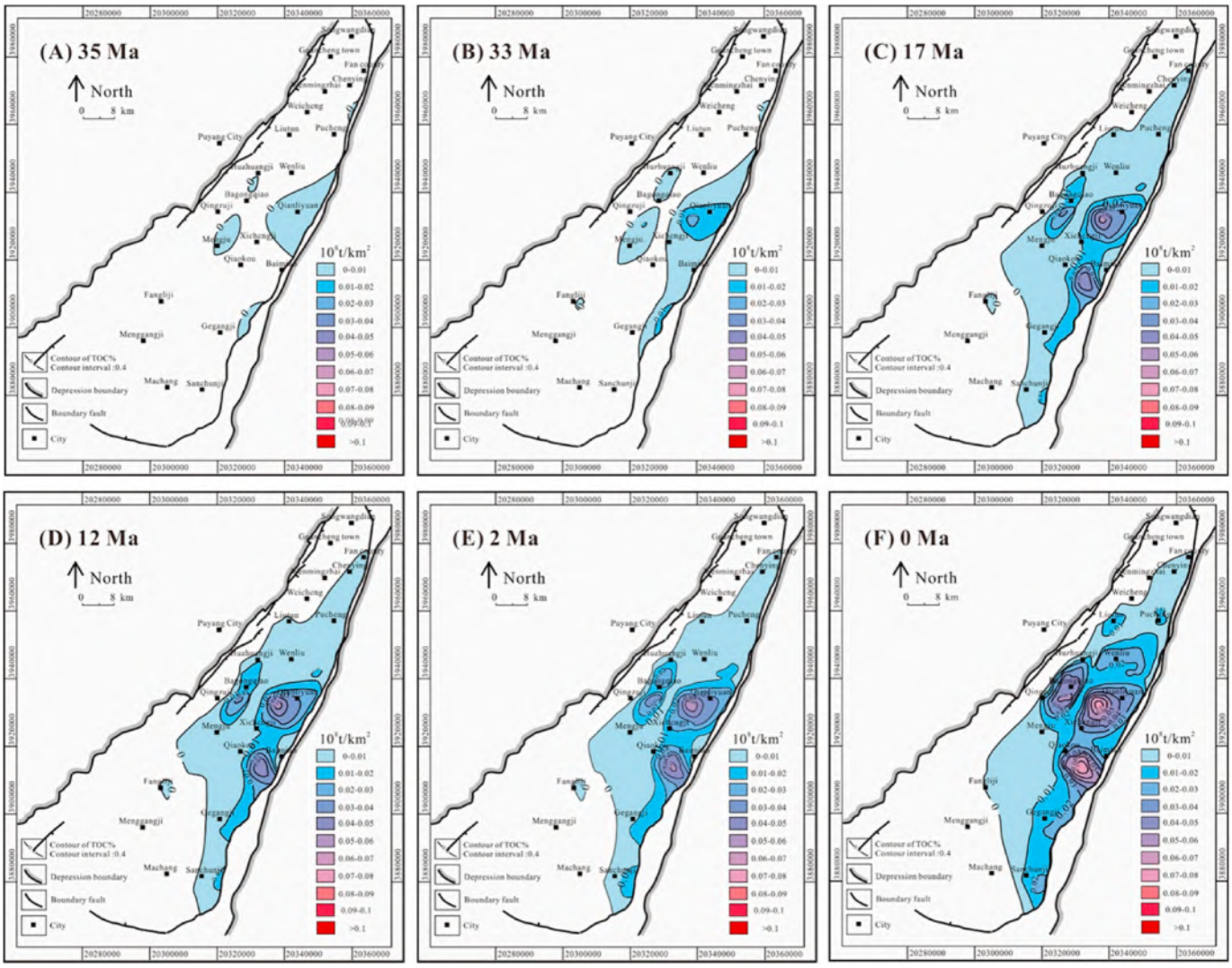

Fig. 23. Hydrocarbon expulsion intensity map of effective source rocks in the upper third submember of the Shahejie Formation in different periods: (A) 33 Ma, (B) 17 Ma, (C) 12 Ma, (D) 2 Ma and (E) modern.

(0.07×10^8 bbl/km^2)). The hydrocarbon expulsion intensity of the Es_1 source rocks has increased gradually. Currently, the accumulated hydrocarbon expulsion amount of the Es_1 source rocks is 0.25×10^8 t (1.83×10^8 bbl) (Fig. 26).

6.3.3. Relative hydrocarbon expulsion contribution of different environments

The relative contribution represents the ratio of hydrocarbon expulsion amount in one sedimentary environment to total hydrocarbon expulsion amount. In general, the depositional period of the Dongying Formation (33-17 Ma) was the main hydrocarbon expulsion period of the source rocks, and it provided hydrocarbon expulsion quantities up to 38.18×10^8 t, which accounted for 55.7% of the current cumulative hydrocarbon expulsion quantity. The relative hydrocarbon expulsion contribution of the transition area was 48.15% at the end of Ed; therefore, this area was the main hydrocarbon expulsion area. In addition, the source rocks had a small amount of hydrocarbon expulsion in the Es_3 (45-35 Ma) and Es_1 (35-33 Ma) periods, which accounted for 5.80% and 16.7% of the cumulative hydrocarbon expulsion quantity, respectively, and the main hydrocarbon expulsion areas were the saline and transition areas. The source rocks had the lowest hydrocarbon expulsion during the deposition of the Guantao Formation (17-12 Ma), accounting for only 1.26% of the cumulative hydrocarbon expulsion quantity. At the end of the N_{1+2}m (2 Ma) period and at present (0 Ma), the hydrocarbon expulsion quantity from the effective source rocks accounted for 8.29% and 12.24% of the cumulative hydrocarbon expulsion quantity, respectively. The main hydrocarbon expulsion formation was still the Es_3^M and Es_3^L source rocks during each period (Fig. 27).

Then, the hydrocarbon expulsion quantity and the relative contribution of the three sedimentary environments in each formation were calculated by the hydrocarbon generation potential method (Table 6). The hydrocarbon expulsion area of Es_4^U source rocks is 232.45 km^2 (89.73 mi^2), and there is only one hydrocarbon expulsion center, which is located in the Qianliyuan area in the north, and the hydrocarbon expulsion quantity is 15.95×10^8 t (116.44×10^8 bbl). Specifically, the saline area has the highest hydrocarbon expulsion amount, with a value of 9.78×10^8 t (71.39×10^8 bbl), and the relative contribution is 61.30% in this formation. The area of hydrocarbon expulsion from the Es_3^L source rocks is 226.45 km^2 (87.41 mi^2), and the location of the hydrocarbon expulsion center remains unchanged, although the area of hydrocarbon expulsion starts to expand. The amount of hydrocarbon expulsion in this formation is 36.44×10^8 t (266.01×10^8 bbl), and the relative contribution of the transition area is 53.64%. The hydrocarbon expulsion area of the Es_3^M source rocks is 235.72 km^2 (90.99 mi^2). The Mengju, Qianliyuan, Liutun and Gegangji areas are hydrocarbon expulsion centers, and abundant hydrocarbons are discharged, with a

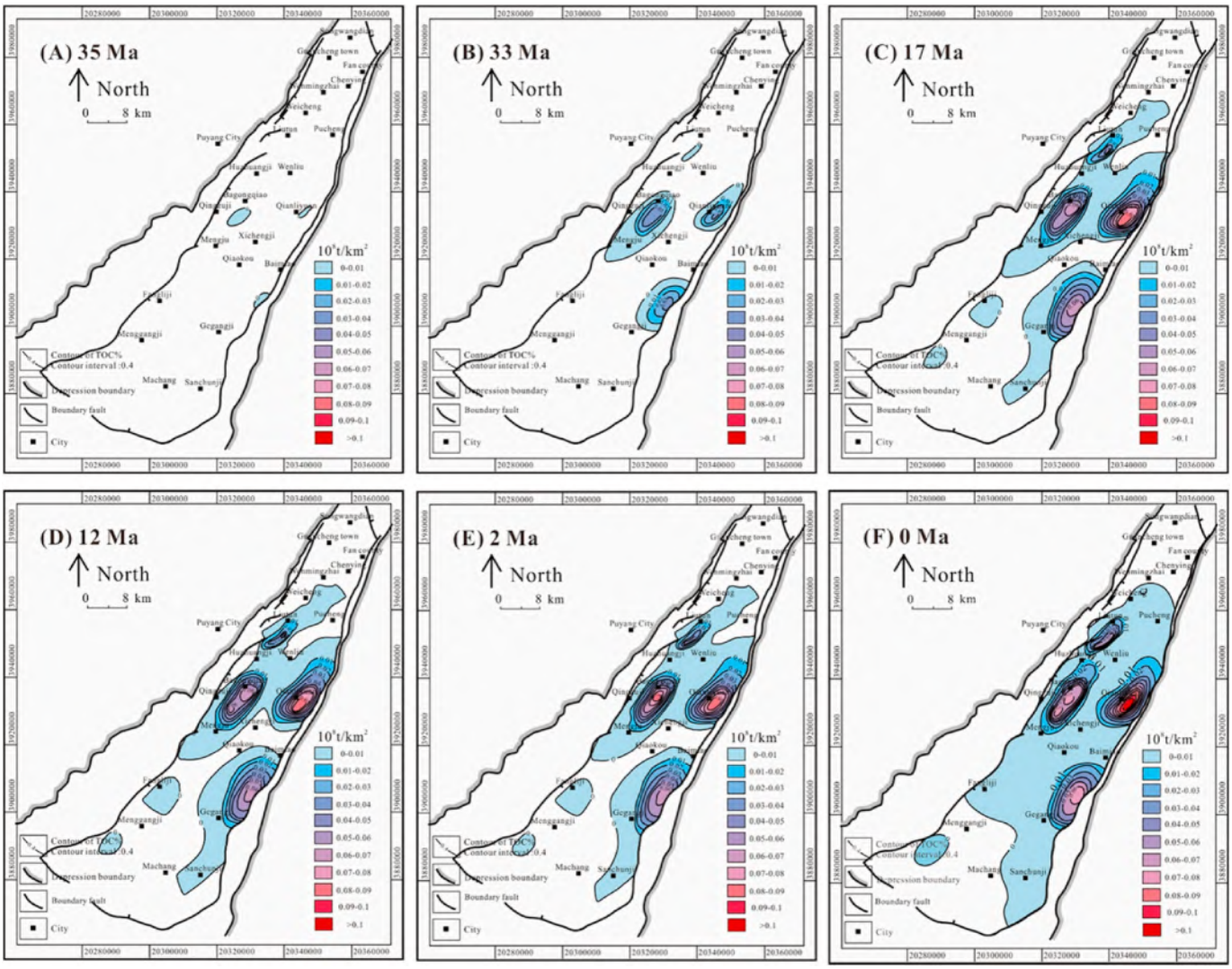

Fig. 24. Hydrocarbon expulsion intensity map of effective source rocks in the middle third submember of the Shahejie Formation in different periods: (A) 35 Ma, (B) 33 Ma, (C) 17 Ma, (D) 12 Ma, (E) 2 Ma and (E) modern.

total hydrocarbon expulsion quantity of 26.63×10^8 t (194.40×10^8 bbl). The transition area of this formation is a main expulsion area, with a hydrocarbon expulsion amount of 14.79×10^8 t (107.97×10^8 bbl), accounting for 55.54% of the total hydrocarbon expulsion amount. The hydrocarbon expulsion area of the Es_3^U source rocks is the same as that of the Es_3^M source rocks, which is 240.67 km^2 (92.90 mi^2), reaching the Puwei area in the north and the Gegangji area in the south. The hydrocarbon expulsion center is located in the Qianliyuan and Mengju areas in the north. The hydrocarbon expulsion quantity of Es_3^U source rocks is 3.77×10^8 t (27.52×10^8 bbl), and that of the transition zone is 3.57×10^8 t (26.06×10^8 bbl), accounting for 94.70% of the hydrocarbon expulsion quantity. The Es_1 source rocks have a small amount of hydrocarbon expulsion, and the hydrocarbon expulsion area is only 34.66 km^2 (13.38 mi^2). The hydrocarbon expulsion center is the same as that of the Es_3^U source rocks, with a hydrocarbon expulsion quantity of 0.25×10^8 t (1.83×10^8 bbl) (Fig. 28).

Overall, the relative contribution of hydrocarbon expulsion in the freshwater area is the lowest in each formation due to the poor quality of the source rocks, poor oil generation capacity and low thickness of the effective source rocks. The contribution of effective source rocks in the saline and transition areas is relatively high. Furthermore, the hydrocarbon expulsion contribution of some formations in the transition area is higher than that in the saline area because the quality of the source rocks in the saline area is excellent, while that of the transition area is only slightly worse. Moreover, the effective source rock is thinner in the saline area due to the development of the pure gypsum-salt rocks. The depositional centers are mostly developed in the transition area; thus, the thickness of the effective source rocks in the transition area is relatively thicker than that in the saline area. Therefore, the amount of hydrocarbon expulsion is slightly higher than that in the saline areas. Generally, the effective source rocks in the saline and transition areas in the Dongpu Depression have a high contribution of hydrocarbon expulsion, and those of the freshwater area have the lowest contribution (Fig. 29).

7. Conclusion

(1) There are five formations of the source rocks in the Paleogene Dongpu Depression, among which the Es_3^M source rocks are the thickest and the Es_1 source rocks are the thinnest. In contrast, the saline areas have the highest organic carbon content, while the freshwater areas have the lowest. Es_3^M and Es_3^L source rocks have a higher TOC content than the other formations. The saline and transition areas are mainly type II_1 and II_2 kerogen, and the

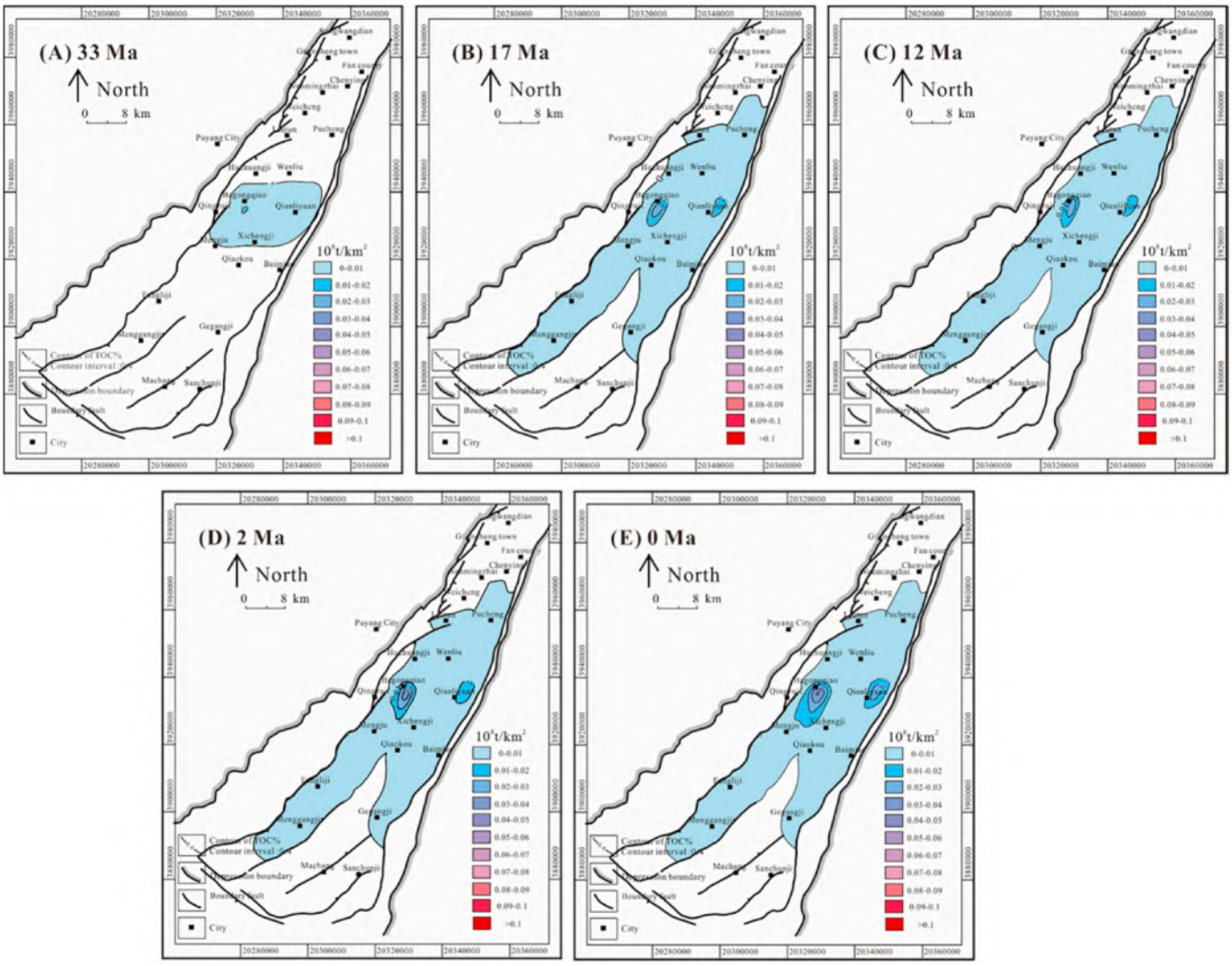

Fig. 25. Hydrocarbon expulsion intensity map of effective source rocks in the lower third submember of the Shahejie Formation in different periods: (A) 35 Ma, (B) 33 Ma, (C) 17 Ma, (D) 12 Ma, (E) 2 Ma and (E) modern.

freshwater areas are mainly type III. The organic matter type in the Es_3 source rocks is developed better than in the other formations. Moreover, most Es_3^M and Es_3^L source rocks have entered the mature stage.

(2) Based on the hydrocarbon generation potential index profile and the S_1/TOC content, the lower limit of effective hydrocarbon source rocks in different sedimentary environments in lacustrine basins was identified for the first time. The lower limits of effective source rocks in the saline, transition and freshwater areas in the Dongpu Depression are TOC values of 0.3%, 0.4% and 0.5%, respectively.

(3) The hydrocarbon expulsion characteristics in different sedimentary environments in the Dongpu Depression are different. The hydrocarbon expulsion thresholds of effective source rocks in the saline, transition and freshwater areas are Ro values of 0.65%, 0.68% and 0.7%, respectively. The effective source rocks in the saline and transition areas have a high hydrocarbon expulsion ratio, although the hydrocarbon expulsion rates and efficiency increase slowly before reaching the peak of hydrocarbon expulsion. The hydrocarbon expulsion rate in the freshwater area is low, although the hydrocarbon expulsion rate and efficiency increase rapidly.

(4) The hydrocarbon expulsion amount is substantially different in different sedimentary environments. Specifically, the hydrocarbon expulsion amount values in the saline, transition and freshwater area are 18.14×10^8 t (132.42×10^8 bbl), 40.77×10^8 t (297.62×10^8 bbl) and 24.13×10^8 t (176.15×10^8 bbl), respectively. The main hydrocarbon expulsion areas are located in the saline and transition areas, and the relative contribution value is 71%. The total hydrocarbon expulsion amount of the five sets of source rocks in the Dongpu Depression is 83.04×10^8 t (606.19×10^8 bbl), and the relative contributions of Es_3^M and Es_3^L source rocks are 32% and 44%, respectively, indicating that the two formations are the main source rock formations. The results of the hydrocarbon expulsion history show that the main peak of hydrocarbon expulsion in the Shahejie Formation of the Dongpu Depression was at the end of Ed (17 Ma).

Credit author statement

Chenxi Zhu: Data curation, Writing - original draft; Fujie Jiang: Structure of the manuscript, Supervision; Pengyuan Zhang: Data curation, Reviewing and Modification; Tao Hu: Reviewing; Ying Liu: Data curation; Tianwu Xu: Data Provider and Reviewing; Yunxian Zhang:

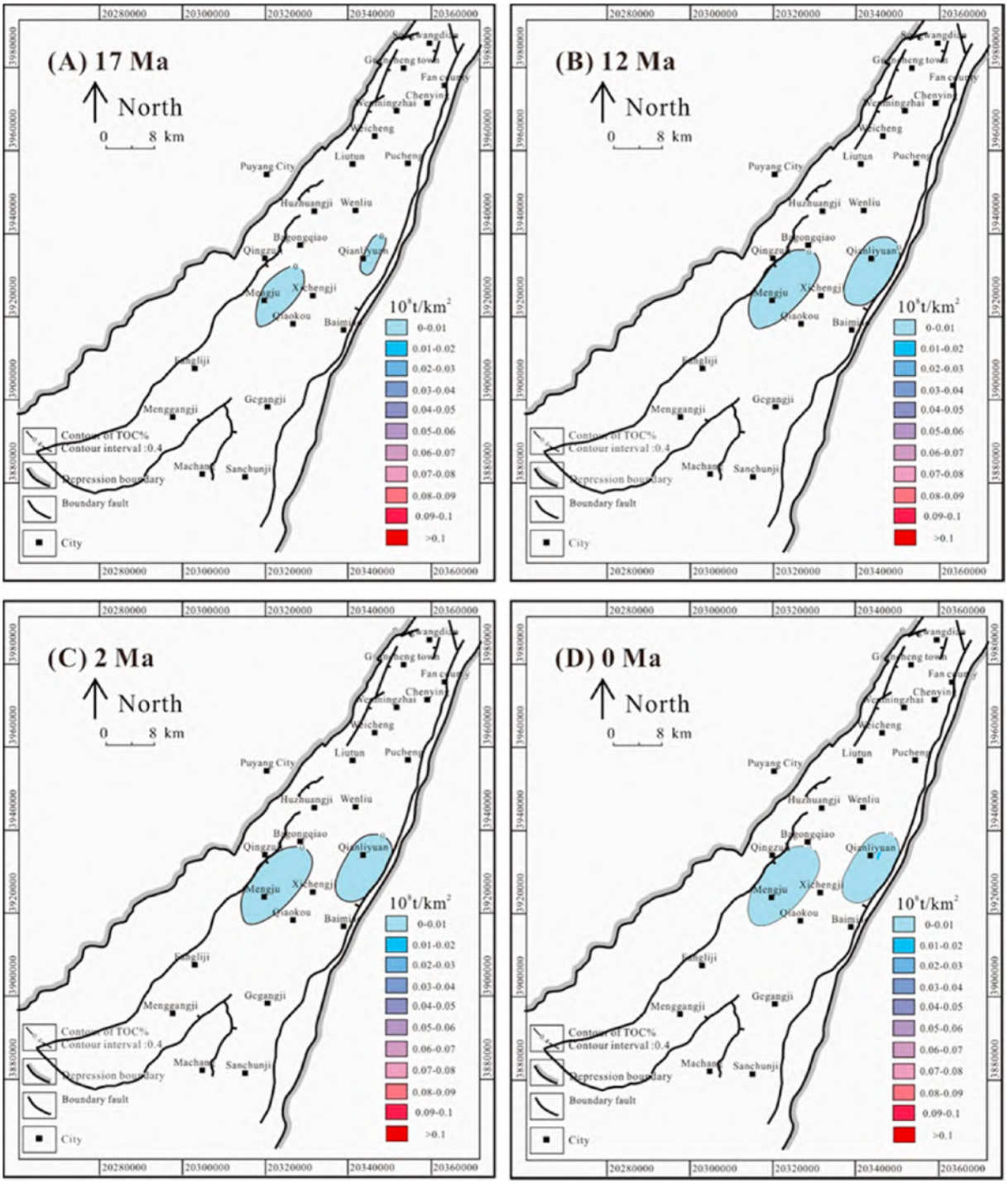

Fig. 26. Hydrocarbon expulsion intensity map of effective source rocks in the upper fourth submember of the Shahejie Formation in different periods: (A) 35 Ma, (B) 33 Ma, (C) 17 Ma, (D) 12 Ma, (E) 2 Ma and (E) modern.

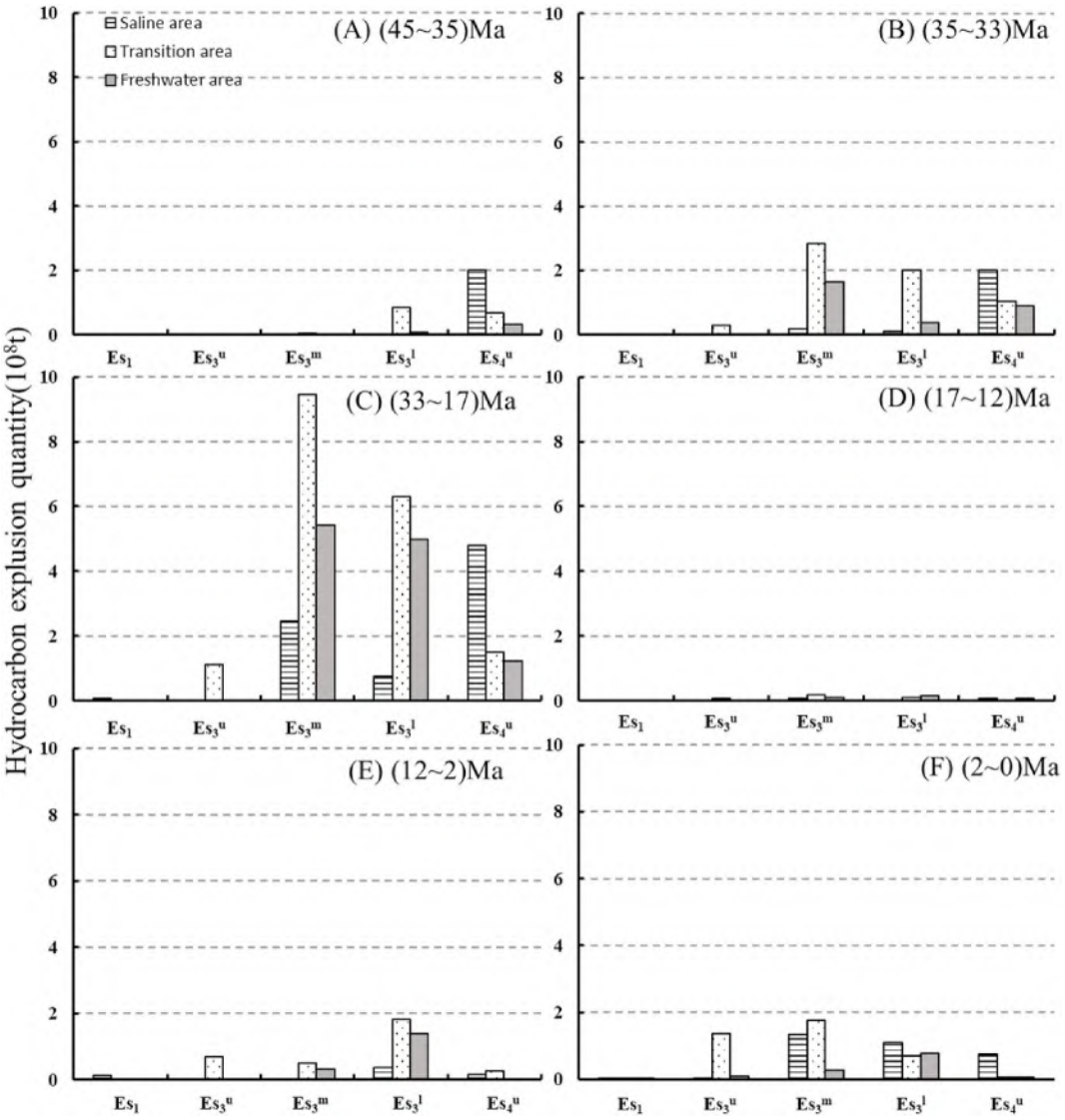

Fig. 27. Hydrocarbon expulsion quantity of effective source rocks in different sedimentary environments during different periods of each formation: (A) 45–35 Ma, (B) 35–33 Ma, (C) 33–17 Ma, (D) 17–12 Ma, (E) 12–2 Ma and (E) 2–0 Ma.

Table 6
Hydrocarbon expulsion amount in different sedimentary environments in different periods (1t = 7.35 bbl).

Geological age (Ma)	35	33	17	12	2	0
Saline area	2.019 × 10^8 t	2.311 × 10^8 t	8.114 × 10^8 t	0.17 × 10^8 t	0.66 × 10^8 t	3.26 × 10^8 t
Transition area	1.573 × 10^8 t	6.205 × 10^8 t	18.38 × 10^8 t	0.36 × 10^8 t	3.29 × 10^8 t	3.92 × 10^8 t
Freshwater area	0.38 × 10^8 t	2.931 × 10^8 t	11.68 × 10^8 t	0.33 × 10^8 t	1.74 × 10^8 t	1.22 × 10^8 t

Data Provider and Reviewing; Qian Deng: Figure processing; Yongshui Zhou: Data Provider; Hang Xiong: Figure processing; Zezhang Song: Reviewing.

Notes

The authors declare no competing financial interest.

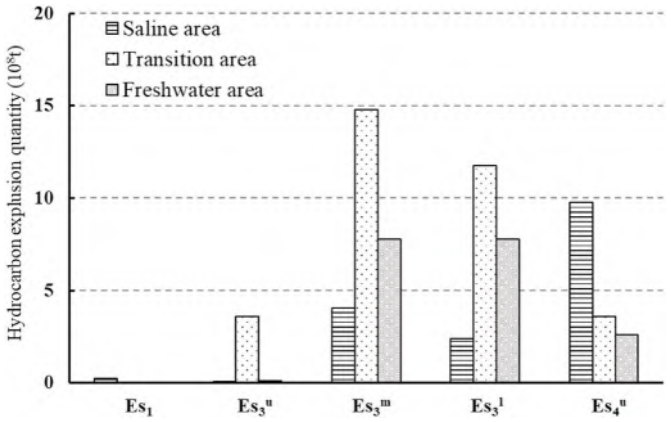

Fig. 28. Hydrocarbon expulsion quantity of effective source rocks in different sedimentary environments of each formation.

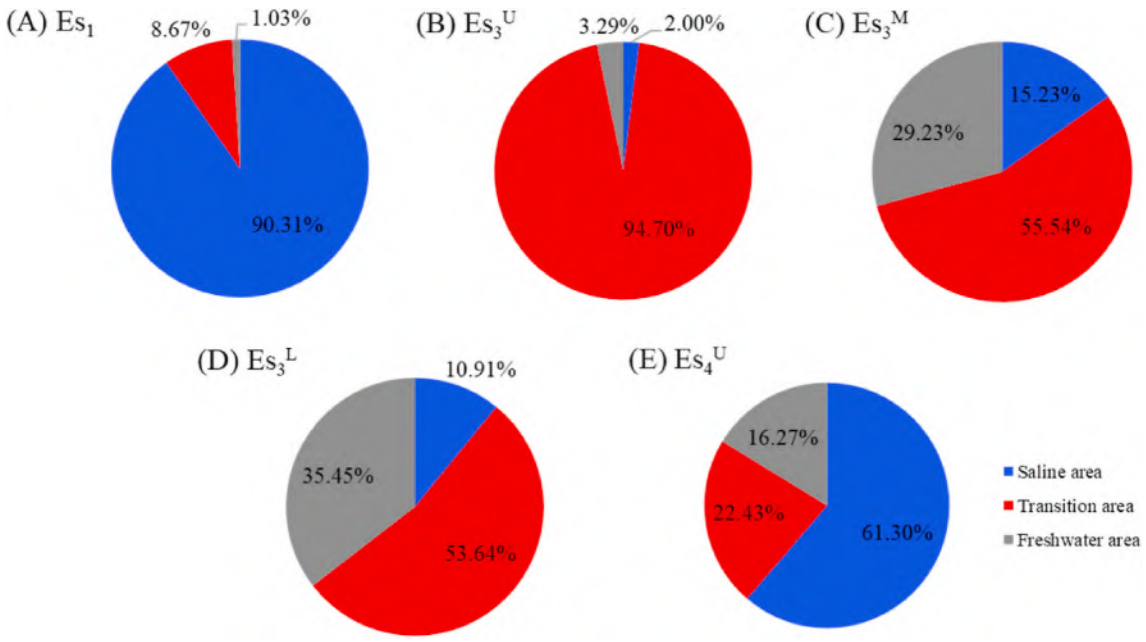

Fig. 29. Relative contribution of hydrocarbon expulsion of effective source rocks in different sedimentary environments of each formation: (A) first member of the Shahejie Formation (Es_1), (B) upper third submember of the Shahejie Formation (Es_3^U), (C) middle third submember of the Shahejie Formation (Es_3^M), (D) lower third submember of the Shahejie Formation (Es_3^L), and (E) upper fourth submember of the Shahejie Formation (Es_4^U).

Declaration of competing interest

The authors declare that they have no known competing financial interests or personal relationships that could have appeared to influence the work reported in this paper.

Acknowledgments

We are grateful to Sinopec Zhongyuan Oilfield Branch for providing experimental data. We express our heartfelt thanks to Haolin Zhou at the University of Alberta for his great help in refining the English language of the manuscript. This research was funded by the National Natural Science Foundation of China (NSFC) (41872128), the Science Foundation of China University of Petroleum,Beijing (No. 2462020YXZZ021), the Youth Program of National Natural Science Foundation of China (Grant NO. 41802148).

Appendix A. Supplementary data

Supplementary data to this article can be found online at https://doi.org/10.1016/j.petrol.2021.108477.

References

Atmaram, M.V., Vivekanand, K., Kumar, S.V., Molloka, B., Damodhar, K.A., Singh, B.D., Subhashree, M., Sadanand, S., Jaywardhan, K., Kumar, V.A., 2018. Evaluation of gas resource potentiality, geochemical and mineralogical characteristics of Permian shale beds of Latehar-Auranga Coalfield, India. Int. J. Coal Geol. 196, 43–62.

Aziz, H.A., Enrique, S.R., Calvo, J.P., Hilgen, F.J., Krijgsman, W., 2003. Palaeoenvironmental reconstruction of a middle Miocene alluvial fan to cyclic shallow lacustrine depositional system in the Calatayud Basin (NE Spain). Sedimentology 50 (2), 211–236.

Bai, H., Pang, X.Q., Kuang, L.C., Pang, H., Wang, X.L., Jia, X.Y., Zhou, L.M., Hu, T., 2017. Hydrocarbon expulsion potential of source rocks and its influence on the distribution of lacustrine tight oil reservoir, Middle Permian Lucaogou Formation, Jimsar Sag, Junggar Basin, Northwest China. J. Petrol. Sci. Eng. 149, 740–755.

Behar, F., Beaumont, V., Penteado, H.L.D., 2001. Rock-Eval 6 technology: performances and developments. Oil & Gas Sci. Technol.-Rev. De L Inst. Francais Du Petrole 56 (2), 111–134.

Bian, L.B., Sanei, H., Niu, Z.C., Yang, D.L., 2020. Geochemical characteristics and origin of petroleum in the southwest complicated fault subsag, Dongpu Depression of China's Bohai Bay Basin. Geol. J. 55 (12), 7858–7871.

Boussafir, M., Gelin, F., Vergès, E.L., Derenne, S., Bertrand, P., Largeau, C., 1995. Electron microscopy and pyrolysis of kerogens from the Kimmeridge Clay Formation, UK: source organisms, preservation processes, and origin of microcycles. Geochem. Cosmochim. Acta 59 (18), 3731–3747.

Cao, Q.Y., 1985. Identification of microcomponents and types of kerogen under transmitted light. Petrol. Explor. Dev. 6 (5), 14–24.

Caplan, M.L., Bustin, R.M., 1999. Palaeoceanographic controls on geochemical characteristics of organic-rich Exshaw mudrocks: role of enhanced primary production. Org. Geochem. 30 (2–3), 161–188.

Chen, J.P., Zhao, C.Y., He, Z.H., 1997. Discussion on evaluation criteria for hydrocarbon generation potential of organic matter in coal measures. Petrol. Explor. Dev. 24 (1), 1–5+91 (in Chinese).

Chen, X.F., Li, S.M., Zhang, H.A., Xu, T.W., Wan, Z.H., Ji, H., Guo, Z.Q., 2018. The controlling effect of paste salt rock on hydrocarbon evolution of source rock and its petroleum geological significance in Dongpu sag. Geoscience 32 (6), 1125–1136 (in Chinese with English abstract).

Chen, Y.C., Shen, Z.M., 2007. Organic Geochemical of Petroleum and Natural Gas. Science Press, Beijing, p. 275.

Damste, J.S.S., Delasheras, F., Deleeuw, J.W., 1992. Molecular analysis of sulfur-rich brown coals by flash pyrolysis-gas chromatography mass-spectrometry - the Type III-S kerogen. J. Chromatogr. A 607 (2), 361–376.

Espitalie, J., Deroo, G., Marquis, F., 1986. Rock-Eval pyrolysis and its applications, 3. Rev. L. Fr. Petrol 41, 73–89.

Fan, B., Shi, L., 2018. Deep-lacustrine shale heterogeneity and its impact on hydrocarbon generation, expulsion, and retention: a case study from the upper triassic Yanchang formation, ordos basin, China. Nat. Resour. Res. 28 (1), 241–257.

Gao, G., Liu, G.D., Fu, J.H., Yao, J.L., 2012. A new method to determine the lower limit of the organic matter abundance of effective source rock – taking the lacustrine argillaceous source rock of Yanchang formation of upper Triassic in Longdong area of ordos basin as an example. J. Xi'an Shiyou Univ. (Nat. Sci. Edn.) 27 (2), 22–26+118 (in Chinese with English abstract).

Guo, J.G., Pang, X.Q., Guo, F.T., Wang, X.L., Xiang, C.F., Jiang, F.J., Wang, P.W., Xu, J., Hu, T., Peng, W.L., 2014. Petroleum generation and expulsion characteristics of Lower and Middle Jurassic source rocks on the southern margin of Junggar Basin, northwest China: implications for unconventional gas potential. Can. J. Earth Sci. 51 (6), 537–557.

Hakimi, M.H., Abdullah, W.H., Mohialdeen, I.M.J., Makeen, Y.M., Mustapha, K.A., 2016. Petroleum generation characteristics of heterogeneous source rock from Chia Gara formation in the Kurdistan region, northern Iraq as inferred by bulk and quantitative pyrolysis techniques. Mar. Petrol. Geol. 71, 260–270.

Hakimi, M.H., Ahmed, A., Kahal, A.Y., Hersi, O.S., Faifi, H.J.A., Qaysi, S., 2020. Organic geochemistry and basin modeling of Late Cretaceous Harshiyat Formation in the onshore and offshore basins in Yemen: implications for effective source rock potential and hydrocarbon generation. Mar. Petrol. Geol. 122, 104701.

Harris, N.B., Freeman, K.H., Pancost, R.D., White, T.S., Mitchell, G.D., 2004. The character and origin of lacustrine source rocks in the Lower Cretaceous synrift section, Congo Basin, west Africa. AAPG (Am. Assoc. Pet. Geol.) Bull. 88 (8), 1163–1184.

He, T.H., Lu, S.F., Li, W.H., Tan, Z.Z., Zhang, X.W., 2018. Effect of salinity on source rock formation and its control on the oil content in shales in the hetaoyuan formation

from the biyang depression, Nanxiang basin, Central China. Energy Fuels 32 (6), 6698–6707.
Hu, Tao, Pang, Xiongqi, Jiang, Shu, et al., 2018. Oil content evaluation of lacustrine organic-rich shale with strong heterogeneity: A case study of the Middle Permian Lucaogou Formation in Jimusaer Sag, Junggar Basin, NW China. Fuel 211, 196–205.
Hu, Tao, Pang, Xiongqi, Jiang, Fujie, et al., 2021. Movable oil content evaluation of lacustrine organic-rich shales: methods and a novel quantitative evaluation model. Earth Sci. Rev.
Hu, T., Pang, X.Q., Jiang, S., Wang, Q.F., Xu, T.W., Lu, K., Huang, C., Chen, Y.Y., Zheng, X.W., 2018. Impact of paleosalinity, dilution, redox, and paleoproductivity on organic matter enrichment in a saline lacustrine rift basin: a case study of Paleogene organic-rich shale in Dongpu depression, bohai Bay Basin, eastern China. Energy Fuel. 32, 5045–5061.
Hu, T., Pang, X.Q., Yu, S., Wang, X.L., Pang, H., Guo, J.G., Jiang, F.J., Shen, W.B., Wang, Q.F., Xu, J., 2015. Hydrocarbon generation and expulsion characteristics of Lower Permian P1f source rocks in the Fengcheng area, northwest margin, Junggar Basin, NW China: implications for tight oil accumulation potential assessment. Geol. J. 51 (6), 880–900.
Huang, D.F., Li, J.C., Zhang, D.J., 1984. Kerogen types and study on effectiveness, limitation and interrelation of their identification parameters. Acta Sedimentol. Sin. 2 (3), 18–33.
Hunt, J.M., 1996. Petroleum Geochemistry and Geology, second ed. W.H. Freeman and Company, New York.
Huo, Z.P., Tang, X., Meng, Q.K., Zhang, J.C., Li, C.R., Yu, X.F., Yang, X., 2020. Geochemical characteristics and hydrocarbon expulsion of lacustrine marlstones in the Shulu sag, bohai Bay Basin, eastern China: assessment of tight oil resources. Nat. Resour. Res. 29, 2647–2669.
Ji, H., Li, S.M., Paul, G., Zhang, H.A., Pang, X.Q., Xu, T.W., He, N.N., Shi, Q., 2018. Geochemical characteristics and significance of heteroatom compounds in lacustrine oils of the Dongpu Depression (Bohai Bay Basin, China) by negative-ion Fourier transform ion cyclotron resonance mass spectrometry. Mar. Petrol. Geol. 97, 568–591.
Jia, C.Z., Zou, C.N., Li, J.Z., Li, D.H., Zheng, M., 2016. Evaluation criteria, major types, characteristics and resource prospects of tight oil in China. Petrol. Res. 1 (1), 1–9.
Jia, J.L., Liu, Z.J., Bechtel, A., Strobl, S.A.I., Sun, P.C., 2013. Tectonic and climate control of oil shale deposition in the upper cretaceous qingshankou formation (Songliao Basin, NE China). Int. J. Earth Sci. 102 (6), 1717–1734.
Jiang, F.J., Pang, X.Q., Jiang, Z.X., Wu, L., Zhou, X.H., Li, X.L., 2010. The quality evaluation and hydrocarbon-expulsion characters of source rocks in the 3rd member of Shahejie Formation in the Bohai Sea. Acta Pet. Sin. 31 (6), 906–912 (in Chinese with English abstract).
Jiang, F.J., Pang, X.Q., Jing, B., Zhou, X.H., Li, J.P., Guo, Y.H., 2016. Comprehensive assessment of source rocks in the Bohai Sea area, eastern China. AAPG (Am. Assoc. Pet. Geol.) Bull. 100 (6), 969–1002.
Klemme, H.D., Ulmishek, G.F., 1991. Effective petroleum source rocks of the world: stratigraphic distribution and controlling depositional factors. AAPG (Am. Assoc. Pet. Geol.) Bull. 75 (12), 1809–1851.
Konyuhov, A.I., Maleki, B., 2006. The Persian Gulf Basin: geological history, sedimentary formations, and petroleum potential. Lithol. Miner. Resour. 41 (4), 344–361.
Kumar, S., Ojha, K., Bastia, R., Garg, K., Das, S., Mohanty, D., 2017. Evaluation of Eocene source rock for potential shale oil and gas generation in north Cambay Basin, India. Mar. Petrol. Geol. 88, 141–154.
Lei, Y.H., Luo, X.R., Zhang, L.K., Vasseur, G., Wang, H.J., Zhao, J.J., 2016. Quantitative assessment of petroleum loss during secondary migration in the Yaojia Formation, NE Songliao Basin, NE China. Mar. Petrol. Geol. 77, 1028–1041.
Liang, C., Jiang, Z.X., Cao, Y.C., Wu, J., Wang, Y.S., Hao, F., 2018a. Sedimentary characteristics and origin of lacustrine organic-rich shales in the salinized Eocene Dongying Depression. Geol. Soc. Am. Bull. 130 (1), 154–174.
Liang, C., Wu, J., Jiang, Z.X., Cao, Y.C., Song, G.Q., 2018b. Sedimentary environmental controls on petrology and organic matter accumulation in the upper fourth member of the Shahejie Formation (Paleogene, Dongying depression, Bohai Bay Basin, China). Int. J. Coal Geol. 186, 1–13.
Liu, J.D., Jiang, Y.L., Tan, Y.M., Mu, X.S., 2014. Relationship between oil and gas in Dongpu sag, bohai Bay Basin. Acta Sedimentol. Sin. 32 (1), 126–137 (in Chinese).
Lu, K., Han, B.Q., Mu, X.S., Cao, H.M., 2011. The paleosedimentary environment of Shahejie Formation in Dongpu Depression and its influence on the abundance of organic matter in source rocks. In: Seminar on Sedimentology and New Techniques and Methods for Oil and Gas Exploration and Development, pp. 133–177.
Lu, S.F., Liu, W., Wang, M., Zhang, L.Y., Wang, Z.T., Chen, G.H., Xiao, D.S., Li, Z.D., Hu, H.T., 2017. Lacustrine shale oil resource potential of e s 3 l sub-member of bonan sag, bohai bay basin, eastern China. J. Earth Sci. 28 (6), 996–1005.
Luo, R., Chen, T., Wang, P., Wang, L.W., 2011. Research on types of organic matter of hydrocarbon source rocks in kongdian formation in weibei depression. J. Chongqing Univ. Sci. Technol. (Nat. Sci. Edn.) 13 (6), 69–71.
Lyu, X.Y., Jiang, Y.L., Liu, J.D., Xu, T.W., Somerville, I., 2019. Geochemical characteristics and hydrocarbon generation potential of the first member of Shahejie Formation (E_2s_1) source rocks in the Dongpu Depression, East China. Geol. J. 54 (4), 2034–2047.
Ma, P.F., Li, Y.L., Wang, C.S., Zheng, L., Lv, D.W., Zou, Y., Li, S., 2018. Oligocene-Miocene source rocks of the Zhongcang Basin: implications for hydrocarbon potential differentiation between lake basins in Central Tibet. Int. J. Coal Geol. 199, 124–137.
Magnier, C., Moretti, I., Lopez, J.O., Gaumet, F., Lopez, J.G., Letouzey, J., 2004. Geochemical characterization of source rocks, crude oils and gases of Northwest Cuba. Mar. Petrol. Geol. 21 (2), 195–214.
Mosmann, R., Falkenhein, F.U.H., Goncalves, A., Nepomuceno, F., 1984. Oil and gas potential of amazon paleozoic basins: abstract. AAPG (Am. Assoc. Pet. Geol.) Bull. 68 (9), 1205.
Mu, X.S., 2011. Mechanism and Model of Salt - Bearing Hydrocarbon Accumulation in Wenliu Area of Dongpu Sag. China University of Geosciences, p. 150.
Mukhopadhyay, P.K., Wade, J.A., Kruge, M.A., 1995. Organic facies and maturation of Jurassic/Cretaceous rocks, and possible oilesource rock correlation based on pyrolysis of asphaltenes, Scotion Basin. Canada. Org. Geochem. 22, 85–104.
Pang, X.Q., 1995. Theory and Application of Hydrocarbon Expulsion Threshold. Petroleum Industry Press, Beijing, China, p. 270.
Pang, X.Q., Li, M.W., Li, S.M., Jin, Z.J., 2005. Geochemistry of petroleum systems in the Niuzhuang south slope of Bohai Bay basin. Part 3. Estimating hydrocarbon expulsion from the Shahejie Formation. Org. Geochem. 36 (4), 497–510.
Peng, J.W., Pang, X.Q., Shi, H.S., Peng, H.J., Xiao, S., 2018. Hydrocarbon generation potential of upper eocene enping formation mudstones in the Huilu area, northern pearl river mouth basin, south China Sea. AAPG (Am. Assoc. Pet. Geol.) Bull. 102, 1323–1342, 07.
Perotti, C., Chiariottil, L., Bresciani, I., Cattaneo, L., Toscani, G., 2016. Evolution and timing of salt diapirism in the Iranian sector of the Persian Gulf. Tectonophysics 679, 180–198.
Peters, K.E., 1986. Guidelines for evaluating petroleum source rock using programmed pyrolysis. AAPG Bull. 70 (3), 318–329.
Peters, K.E., Cassa, M.R., 1994. Applied source rock geochemistry. Mem. Am. Assoc. Petrol. Geol. 93–117.
Peters, K.E., Walters, C.C., Mankiewicz, P.J., 2006. Evaluation of kinetic uncertainty in numerical models of petroleum generation. AAPG (Am. Assoc. Pet. Geol.) Bull. 90 (3), 387–403.
Peters, K.E., Walters, C.C., Moldowan, J.M., 2005. The biomarker guide. In: Biomarkers &Isotopes in Petroleum Systems & Earth History, vol. 2, p. 490.
Petersen, H.I., Tru, V., Nielsen, L.H., Duc, N.A., Nytoft, H.P., 2006. Source rock properties of lacustrine mudstone and coals (oligocene Dong Ho formation), onshore Song Hong basin, northern vietnam. J. Petrol. Geol. 28 (1), 19–38.
Pu, B.L., Dong, D.Z., Zhao, J.Z., Chuang, E.R., Huang, J., 2015. Differences between marine and terrestrial shale gas accumulation: taking longmaxi shale sichuan Basin and Yanchang shale ordos basin as example. Acta Geol. Sin. 89 (A01), 200–206.
Ribes, C., Kergaravat, C., Crumeyrolle, P., Lopez, M., Bonnel, C., Poisson, A., Kavak, K.S., Callot, J.P., Ringenbach, J.C., 2015. Factors controlling stratal pattern and facies distribution of fluvio-lacustrine sedimentation in the Sivas mini-basins, Oligocene (Turkey). Basin Res. 29, 596–621.
Shao, X.H., Pang, X.Q., Li, H., Hu, T., Xu, T.W., Xu, Y., Li, B.Y., 2018. Pore network characteristics of lacustrine shales in the Dongpu Depression, Bohai Bay Basin, China, with implications for oil retention. Mar. Petrol. Geol. 96, 457–473.
Shen, J.N., Yang, J.Y., Zhou, F., Zhang, J., Yang, G.N., Qiu, Y.P., Sun, Y., 2013. Study of kerogen type index through the calculation of organic elements. J. Northeast Petrol. Univ. 37 (5), 24–31.
Si, W., Hou, D.J., Wu, P., Zhao, Z., Ma, X.X., Zhou, H.F., Cao, L.Z., 2020. Geochemical characteristics of lower cretaceous lacustrine organic matter in the southern sag of the Wuliyasitai depression, Erlian Basin, China-ScienceDirect. Mar. Petrol. Geol. 118, 104404.
Smith, J.W., Beard, T.N., Trudell, L.G., 1978. Colorado's Primary Oil-Shale Resource for Vertical Modified In-Situ Processes. Green River Formation, 1978.
Sykes, R., Snowdon, L.R., 2002. Guidelines for assessing the petroleum potential of coaly source rocks using Rock-Eval pyrolysis. Org. Geochem. 33 (12), 1441–1455.
Tang, L., Pang, X.Q., Song, Y., Jiang, Z.X., Jiang, S., Li, Q.W., Zhang, H.A., Yang, Y.D., Li, X.H., 2019. Lower limit of hydrocarbon generation in source rocks: a case study from the Dongpu Depression, Bohai Bay Basin, East China[J]. J. Asian Earth Sci. 182 (15).
Thiry, M., 1989. Geochemical evolution and paleoenvironments of the eocene continental deposits in the Paris Basin. Palaeogeogr. Palaeoclimatol. Palaeoecol. 70 (1–3), 0-163.
Tissot, B., Welte, D., 1980. Petroleum formation and occurrence. Earth Sci. Rev. 16, 372–373 (Springer-Verlag).
Tissot, B.P., 1987. Thermal history of sedimentary basins, maturation indices, and kinetics of oil and gas generation. AAPG (Am. Assoc. Pet. Geol.) Bull. 71, 1445–1466.
Tissot, B.P., Welte, D.H., 1984. Petroleum Formation and Occurrence, second ed. Springer-Verlag Berlin Heidelberg, p. 702.
Tu, J.Q., Wang, S.Z., Fei, C.D., 1998. Classification of organic maceral components of kerogen under transmission light and fluorescence. Petrol. Explor. Dev. 2, 27–29 (in Chinese).
Van Krevelen, D.W., 1961. Coal. Elsevier Science, New York, p. 514.
Wang, Y.M., Niu, J.Y., Qiao, H.S., Cui, W.Q., 2002. Analysis and understanding of the oil and gas resource potential in the deep layer of Bohai Bay Basin. Petrol. Explor. Dev. 2, 21–25 (in Chinese).
Wang, E.Z., Liu, G.Y., Pang, X.Q., Li, C.R., Zhao, Z.F., Feng, Y., Wu, Z.Y., 2020c. An improved hydrocarbon generation potential method for quantifying hydrocarbon generation and expulsion characteristics with application example of Paleogene Shahejie Formation, Nanpu Sag, Bohai Bay Basin. Mar. Petrol. Geol. 112, 104106.
Wang, J.B., Gao, Z.Q., Kang, Z.H., Zhu, D.Y., Liu, Q.Y., Ding, Q., Liu, Z.W., 2019. Geochemical characteristics, hydrocarbon potential and depositional environment of the Yangye Formation source rocks in Kashi sag, southwestern Tarim Basin, NW China. Mar. Petrol. Geol. 112, 104084.
Wang, M., Sherwood, N., Li, Z., Lu, S., Wang, W., Huang, A., Peng, J., Lu, K., 2015. Shale oil occurring between salt intervals in the Dongpu depression, bohai Bay Basin. China. Int. J. Coal Geol. 152 (1), 100–112.

Wang, Q.F., Jiang, F.J., Ji, H.C., Jiang, S., Guo, F.X., Gong, S.Y., Wang, Z., Liu, X.H., Li, B. S., Chen, Y.Y., Deng, Q., 2020a. Differential enrichment of organic matter in saline lacustrine source rocks in a rift basin: a case study of Paleogene source rocks, Dongpu depression, bohai Bay Basin. Nat. Resour. Res. 29 (6), 4053–4072.

Wang, Q.F., Jiang, F.J., Ji, H.C., Jiang, S., Liu, X.H., Zhao, Z., Wu, Y.Q., Xiong, H., Li, Y., Wang, Z., 2020b. Effects of paleosedimentary environment on organic matter enrichment in a saline lacustrine rift basin - a case study of Paleogene source rock in the Dongpu Depression, Bohai Bay Basin. J. Petrol. Sci. Eng. 195, 107658.

Wei, W., Algeo, T.J., Lu, Y.B., Lu, Y.C., Liu, H.M., Zhang, S.P., Peng, L., Zhang, J.Y., Chen, L., 2018. Identifying marine incursions into the Paleogene Bohai Bay Basin lake system in northeastern China. Int. J. Coal Geol. 200, 1–17.

Weng, F.F., Shi, X.G., 2010. Analysis on exploration potential of E_1f_3 oil reservoir in Yancheng sag, Subei Basin. Compl. Hydrocarb. Reserv. 3 (4), 14–17+27.

Wu, X.L., Lu, F.C., Zhang, Y.X., Tang, W.Z., 2000. Geochemical characteristics of hydrocarbon source rock and oil and gas in pushen 8 well, Dongpu sag. Petrol. Explor. Dev. 27 (5), 32-35+19-8 (in Chinese).

Yang, J.K., Li, W.L., Gao, S.Y., Zhang, J.L., Zhang, Y., Lu, J.W., 2019. Sedimentology, geological modeling and prediction of the remaining oil distribution in a complicated fault-block reservoir in the Weicheng Oilfield, Dongpu Depression, China. Geosci. J. 23 (5), 791–804.

Yang, W.L., Li, Y.K., Gao, R.Q., Guo, Q.F., 1981. Organic matter types and its evolution model of lacustrine source rocks of Songliao Basin. Sci. China 18 (1), 1000–1008 (in Chinese with English abstract).

Yue, B.S., Huang, H., Chen, B., Zhou, J.H., Yu, B.T., 2005. Evaluation method and application of logging source rock in Dongpu sag. J. Oil Gas Technol. (J. Jianghan Petroleum Inst.) 27 (3), 351–354+270 (in Chinese).

Yurchenko, I.A., Moldowan, J.M., Peters, K.E., Magoon, L.B., Graham, S.A., 2018. Source rock heterogeneity and migrated hydrocarbons in the Triassic Shublik Formation and their implication for unconventional resource evaluation in Arctic Alaska. Mar. Petrol. Geol. 92, 932–952.

Zhang, P.Y., Jiang, F.J., Zhu, C.X., Huang, R.D., Hu, T., Xu, T.W., Li, W.D., Xiong, H., 2021. Gas Generation Potential and Characteristics of Oil-Prone Shale in the Saline Lascutrine Rifting Basins: A Case Study of the Dongpu Depression, Bohai Bay Basin. Energy & Fuels.

Zhao, J.Z., 2001. The Cambrian-Ordovician Marine source rocks in the north of Tarim basin are re-recognized. Acta Sedimentol. Sin. 19 (1), 117–124 (in Chinese).

Zhao, Q.M., Yang, D.Q., Jiang, J.G., Peng, J., Xu, S.Z., Organic geochemistry and sedimentary environment of the Tertiary salt-lake facies in Wuyang and Xiangcheng depression. Acta Sedimentol. Sin.. 21 (2), 334-339 (in Chinese).

Zheng, D.Y., Pang, X.Q., Ma, X.H., Li, C.R., Zheng, T.Y., Zhou, L.M., 2019. Hydrocarbon generation and expulsion characteristics of the source rocks in the third member of the upper triassic xujiahe formation and its effect on conventional and unconventional hydrocarbon resource potential in the sichuan basin. Mar. Petrol. Geol. 109, 175–192.

Zheng, Z.Y., Zuo, Y.H., Jiang, S., Zhou, Y.S., Zhang, Y.X., Wu, W.T., Yan, K.N., Yang, M. H., 2020. Carbon isotope kinetics effect on the natural gas accumulation: a case study of the baimiao area, Dongpu depression, north China. Energy Fuels 34 (2), 1608–1619.

Zhu, G.Y., Jin, Q., 2003. Geochemical characteristics of two sets of excellent source rocks in Dongying depression. Acta Sedimentol. Sin. 21 (3), 506–512 (in Chinese with English abstract).

Zhu, X.J., Chen, J.F., Li, W., Pei, L.X., Liu, K.X., Chen, X.D., Zhang, T.L., 2020. Hydrocarbon generation potential of Paleogene coal and organic rich mudstones in Xihu sag, East China Sea Shelf basin, offshore eastern China. J. Petrol. Sci. Eng. 184, 106450.

Zhu, Y.M., Chen, S.B., Lan, X.D., Wang, M., Fang, J.H., 2010. Hydrocarbon generation evaluation of Permo-Carboniferous source rocks in Qinggu-2 well in Dongpu depression. J. Earth Sci. 21, 94–103.

Zou, C.N., Guo, Q.L., Yang, Z., Wu, S.T., Chen, N.S., Lin, S.H., Pan, S.Q., 2019. Resource potential and core area prediction of lacustrine tight oil: the Triassic Yanchang Formation in Ordos Basin, China. AAPG (Am. Assoc. Pet. Geol.) Bull. 103 (6), 1493–1523.

Zuo, Y.H., Tang, S.L., Zhang, W., Zhang, Y.X., Xin, Y.P., Zhou, Y.S., 2017. Cenozoic tectono-thermal history of Dongpu sag. Earth Sci. Front. 24 (3), 149–156 (in Chinese with English abstract).